

**University of Natural Resources and
Life Sciences Vienna**

Department of Biotechnology



VIBT
Vienna Institute
of BioTechnology

Regulation and detection of dietary miR-21 in mice

Masterarbeit

zur Erlangung des akademischen Grades
Diplom-Ingenieur

Adnan Becirovic, BSc.

Vorstand:

Betreuer: Assoc.Prof. Dr. Johannes Grillari

Mitbetreuerin: Regina Weinmüller, MSc.

Eidesstaatliche Erklärung

Ich erkläre eidesstattlich, dass ich die Arbeit selbständig angefertigt, keine anderen als die angegebenen Hilfsmittel benutzt und alle aus ungedruckten Quellen, gedruckter Literatur oder aus dem Internet im Wortlaut oder im wesentlichen Inhalt übernommenen Formulierungen und Konzepte gemäß den Richtlinien wissenschaftlicher Arbeiten zitiert und mit genauer Quellenangabe kenntlich gemacht habe.

Wien, _____

Unterschrift

Danksagung

Der erste und größte Dank geht an die gesamte Arbeitsgruppe der Grillari Labs und insbesondere an meine liebevolle Betreuerin Regina Weinmüllner für diese spannende und lehrreiche Zeit am Department für Biotechnologie der BOKU Wien – trotz Kinderstress und dementsprechend wenig Schlaf hatte Regina immer ein offenes Ohr und hilfreiche Ratschläge für mich parat – alleine die Experimente mit den 3D-Hautäquivalenten werden ewig in meiner Erinnerung bleiben (Stichwort: Wachshose). Es ist sicherlich kein leichtes Unterfangen, sowohl im privaten als auch im beruflichen Leben so viel Geduld beweisen zu müssen und immer noch diese Freundlichkeit auszustrahlen! **Vielen Dank für alles, liebe Regina!**

Außerdem wären meine ersten Schritte in der medizinischen Forschung durch die tatkräftige Unterstützung und Tipps solch enthusiastischen Mentoren wie Markus Schosserer, Fabian Nagelreiter, Ingo Lämmermann, Clemens Heissenberger und allen anderen Mitgliedern der Laborgruppe keine solche Leichtigkeit gewesen. Das großartige und inspirierende Arbeitsklima ist keine Selbstverständlichkeit in dieser Branche und ist sicherlich ein Teil des Erfolgsrezeptes dieser Arbeitsgruppe! Dafür gebührt den Kollegen der größte Respekt und Dank!

Natürlich gebührt dieses auch dem wissenschaftlichen *Mastermind* der Arbeitsgruppe, Johannes „Giovanni“ Grillari, der trotz vieler Reises Strapazen rund um Konferenzen und Co. es nicht dem Zufall überlassen hat, dass die Grillari Labs einen hervorragenden Ruf in der Welt der Altersforschung etablieren konnten. Auch für die Möglichkeit, meine ersten Erfahrungen am Mausmodell zu sammeln und auf dem Gebiet der mikro-RNAs Fuß fassen zu können, möchte ich mich an dieser Stelle sehr herzlich bedanken. Hierbei möchte ich mich vor allem auch bei den Mitarbeitern des BOKU-Spinoffs *TAmiRNA* bedanken, die mir mit ihrer Expertise im Bereich der mikro-RNAs tatkräftig unter die Arme gegriffen haben.

Meinen Dank möchte ich außerdem den Kollegen der Medizinischen Universität Wien aussprechen, die sowohl meine rechte Hand bei der Vorbereitung, Durchführung und Interpretation der Mausexperimente waren – hervorheben möchte ich hier insbesondere Ass.Prof. Petra Heffeter und den Tierpfleger Gerhard Zeitler.

Zu guter Letzt schulde ich natürlich auch meiner großartigen Familie einen herzlichen Dank. Durch die hundertprozentige Rückendeckung konnte ich mich vollends auf mein Studium fokussieren. Auch ließen sie sich nicht durch vereinzelt Rückschläge aus der Ruhe bringen und pushten mich weiter, meiner Hingabe zur Biotechnologie nachzugehen.

Vielen herzlichen Dank und ich wünsche euch allen viel Glück auf eurem weiteren Lebensweg und vor allem viel Erfolg für eure Experimente!

Abstract

In recent years, the study of micro-RNAs (miRNA) as biomarkers and post-transcriptional regulation factors has become more important as countless diseases might arise due to varying levels of certain micro-RNA families in the organism. Some hypotheses claim that uptake of dietary micro-RNAs into the human body might lead to extrinsic growth stimulation and eventually to tumorigenic effects. In this master thesis, we wanted to identify if dietary miRNA-21, a known oncogenic miRNA, is taken up into the organism by the gastric tract after feeding either miR21 knockout or wild type mice with miRNA-containing cow milk. As starting point, we first confirmed data from literature that there is indeed an influence of milk processing techniques on miRNA content. This leads to a substantially higher micro-RNA 21 content in unprocessed pasteurized cow milk than in ultra-high-temperature milk.

With these results in mind, we decided to design an altering feeding scheme between unprocessed and UHT milk and analyzed the miRNA-21 concentration by highly sensitive methods like qPCR in mouse blood and organs at different timepoints throughout the experiment. Interestingly, we could not show any significant increase of miRNA-21 levels in the mouse, regardless of the milk fed. Hence, our results may help to tone down some opinions that the consumption of cow milk might increase the risk of oncologic diseases for humans.

Kurzfassung

In den letzten Jahren haben Untersuchungen von mikro-RNAs (miRNA) als Biomarker und post-transkriptionelle Faktoren an Wichtigkeit zugenommen, da eine große Anzahl von Krankheiten durch schwankende Konzentrationen von speziellen mikro-RNA Familien im Organismus ausgelöst werden können. Manche Hypothesen stellen die Möglichkeit in den Raum, dass die Aufnahme von diätischen mikro-RNAs in den menschlichen Körper extrinsische Effekte wie Wachstumsstimulation und Tumorbildung auslösen kann.

Im Rahmen dieser Masterarbeit haben wir die Resorption einer speziellen onkogenen mikro-RNA, miR-21, durch den Gastrointestinaltrakt nach Fütterung von miR-21 Knockout und Wildtyp Mäusen mit mikro-RNA enthaltender Kuhmilch untersucht. In ersten Experimenten zeigte sich in Übereinstimmung mit Literaturdaten, dass die der Prozess zur Haltbarmachung einen großen Einfluss auf die mikro-RNA Konzentration in der Milch hat. Pasteurisierte Kuhmilch wies eine substanziiell höhere mikro-RNA 21 Konzentration auf als ultrahocherhitzte Haltbarmilch (UHT).

Anhand dieser Daten entwarfen wir einen Fütterungsplan für unser Experiment und analysierten nach abwechselnder Gabe von pasteurisierter und UHT-Milch durch hochsensitive Methoden wie qPCR die mikro-RNA 21 Konzentration in Mäuseblut und -organen zu verschiedenen Zeitpunkten. Interessanterweise konnten wir, unabhängig von der Art der gefütterten Milch, keinen signifikanten Anstieg von mikro-RNA 21 in den Mäusen feststellen. Ein Zusammenhang zwischen Kuhmilchkonsumation und einem erhöhten Risiko für Krebserkrankungen durch Aufnahme von diätischer mikro-RNA 21 erscheint daher aufgrund unserer Datenlage als eher unwahrscheinlich.

Table of Content

1. Introduction	1
1.1. What are micro-RNAs?	1
1.2. Biogenesis of micro-RNAs	2
1.3. Mode of action of micro-RNAs	3
1.4. Extracellular circulating micro-RNAs as means of communication	5
1.5. Micro-RNAs as biomarkers	7
1.5.1. Difference between human blood and serum	9
1.5.2. How to determine the hemolytic effect in blood samples?	9
1.6. Introducing a special family of micro-RNAs: oncomiRs	10
1.6.1. miR-17~92 polycistron	11
1.6.2. miR-155	12
1.6.3. miR-21	15
1.6.3.1. PI3K-Akt pathway	15
1.7. Milk – only nutritional or also functional value?	17
2. Aim	19
3. Material and Methods	20
3.1. Materials	20
3.1.1. Disposables	20
3.1.2. Equipment	21
3.1.3. Chemicals	21
3.1.4. Primers	22
3.2. Methods	22
3.2.1. Mouse breeding	22
3.2.2. Mouse feed and experimental timeline	24
3.2.3. Mouse organ harvest	25
3.2.4. Murine blood preparation	25
3.2.5. RNA-isolation from biofluids (serum, plasma, milk)	26
3.2.6. RNA isolation from tissue (organs)	27
3.2.7. Heparinase treatment of total RNA	27
3.2.8. Complementary DNA (cDNA) synthesis	28
3.2.9. Real-time quantitative polymerase chain reaction (RT-qPCR)	29
3.2.10. Statistics	31
4. Results	32
4.1. miR-21 quantification in pasteurized and ultra-high-temperature treated milk	32
4.2. Mouse genotyping miR-21	34
4.3. Animal feeding experiment	36
4.3.1. Negative effects of heparin on qPCR	36
4.3.2. Analysis of uptake of miR-21 into the murine bloodstream	38
4.3.3. Analysis of miR-21 uptake in liver and small intestine	40
5. Discussion	43

5.1. Summary, key messages and questions	43
5.2. Outlook on experimental setup improvements and contrasting approaches in the study of miRNA-uptake	44
6. <i>References</i>	47
7. <i>Appendix</i>	<i>i</i>
7.1. Abbreviations	<i>i</i>

1. Introduction

1.1. What are micro-RNAs?

The discovery of the first micro-RNA, *lin-4*, in 1993 by the research groups of Ambros (Lee, Rhonda, Feinbaum, & Ambros, 1993) and Ruvkun (Wightman, Ha, & Ruvkun, 1993) in *Caenorhabditis elegans* has been a milestone in the fields of DNA expression, regulation and study of inter- and intracellular communication and has shed new light on the mechanisms of gene regulation.

Nowadays, after years of intensive study, micro-RNAs (miRNA) are widely accepted as important post-transcriptional regulation factors. They can either dampen or completely nullify the expression of a target gene after its transcription to mRNA which consequently influences many biological processes in the organism (Martin & Caplen, 2007). Micro-RNAs are single-stranded, 19-24 nucleotides long, non-coding and are found to be highly conserved through many species showing homology even between the plant and animal world (Bartel, 2004). They are indistinguishable from another class of small nucleic acids, the small interfering RNAs (siRNA). Both have the same length, possess 5' phosphate and 3' hydroxyl ends and mediate target gene expression by assembling into the RISC (RNA induced silencing complex) but deviate from each other based on their origins and biogenesis (Kim, 2005).

Predictions suggest that around 3% of all human genes account for micro-RNAs that target around 30% of protein encoding genes. This emphasizes the vast amount of possible interactions on post-transcriptional level in organisms (Bentwich, 2005). Also, the possibility of utilizing micro-RNAs as validated biomarkers for many age-associated diseases has arisen, especially after the discovery that some micro-RNAs target tumor suppressor genes (Smith-Vikos & Slack, 2012).

Furthermore, micro-RNAs usually derive from clusters on the genome. They are transcribed as a single long transcript with a unique seed (target) region and are summarized as members belonging to a distinct "family" depending on their origin (Tanzer

& Stadler, 2004). Due to the single-target mechanism, the study of these families has become more important in recent years.

In the next few chapters, the details on biogenesis and mode of action of micro-RNAs are discussed while also showcasing the most prominent micro-RNA members and their effect on human health.

1.2. Biogenesis of micro-RNAs

The canonical way of biogenesis and maturation of micro-RNAs can be visually studied in *Figure 1* and begins with the transcription of the specific miRNA gene into a 1 kb pri-miRNA transcript by pol II. After subsequent nuclear cleavage by Drosha RNase II endonuclease, an approximately 70 nt long stem-loop precursor (pre-miRNA) (Lee Y. , 2002) is created. This pre-miRNA is then actively transported by Ran-GTP through the exportin-5 receptor into the cytoplasm where the final maturation occurs by removal of the terminal loop by the RNase III endonuclease complex Dicer (E Lund, 2004). The nascent miRNA duplex is then separated by TAR-RNA binding protein (TRBP) into the 3'-5' (+)-strand (guide miRNA) and 5'-3' (-)-strand (passenger miRNA). In the following step, the first strand can interact with the Argonaute (AGO) family of proteins in an ATP-dependent manner forming the RNA silencing complex (RISC) while the passenger strand is degraded due to its thermodynamical instability (Yoda, 2010).

Additionally, micro-RNA transcription and biogenesis can occur through a non-canonical pathway, which includes Dicer-independent and Drosha-independent pathway variants (Ruby, Jan, & Bartel, 2007), but this thesis will focus on the dominant canonical pathway and its miRNA products.

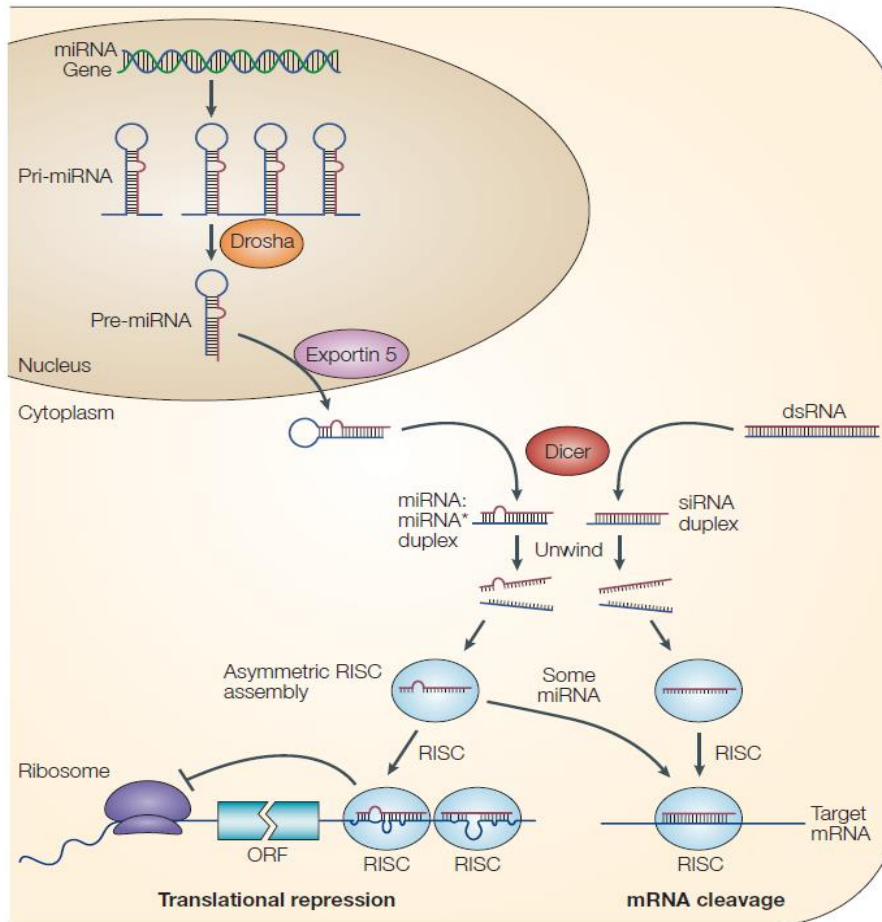


Figure 1: Maturation process and mode of action of micro-RNAs: After cleavage by Drosha and export to the cytosol by exportin-5, the pre-miRNA is further processed in the cytoplasm by Dicer and other factors. The mature miRNA can then interact with the RISC complex and commit to either translational repression or mRNA cleavage (He & Hannon, 2004)

1.3. Mode of action of micro-RNAs

After guide strand loading onto the RISC complex and formation of the miRISC protein bundle in the cytoplasm, micro-RNAs can suppress gene expression. This is accomplished by binding of the miRISC at the 3'UTR (untranslated) region of the target mRNA on the so-called miRNA response elements (MRE) – however unlike with siRNA-mediated silencing, where full complementarity between seed region and guide strand is necessary, the complementarity level in miRNA-dependent silencing may vary. Depending on the complementarity level, the process of gene silencing may either be realized by AGO2-dependent slicing or miRISC-mediated translational inhibition.

The first requires full miRNA:MRE complementarity for the initiation of the endonuclease activity of AGO2 (Jo, 2015). However, imperfect match between miRNA and MRE dissociates the AGO2 protein from the silencing complex leading to the recruitment of the GW182 family of proteins. The interaction between GW182 and the miRISC facilitates deadenylation and in consequence decapping by DCP2 (decapping protein 2), followed by 5'-3' degradation by exoribonuclease 1 (XRN1) of the target mRNA (JE Braun, 2012).

Nonetheless, this efficient mechanism of post-transcriptional gene silencing may not be limited to the cytoplasm as another study has shown: In senescent (growth arrested and non-replicating) human fibroblasts, nuclear AGO2 acts as the effector protein for miR-guided-senescence-associated target gene silencing (SA-TGS) and cooperates with Retinoblastoma protein (Rb) in the stable repression of certain target EF2 genes (elongation factor 2) (Figure 2). This extends the common theory of cytosolic post-transcriptional gene silencing (PTGS) to nuclear TGS and highlights how micro-RNAs (in this case *let-7*) function as important executors of essential biological processes like cellular senescence and tumor suppression (Benhamed, 2012)

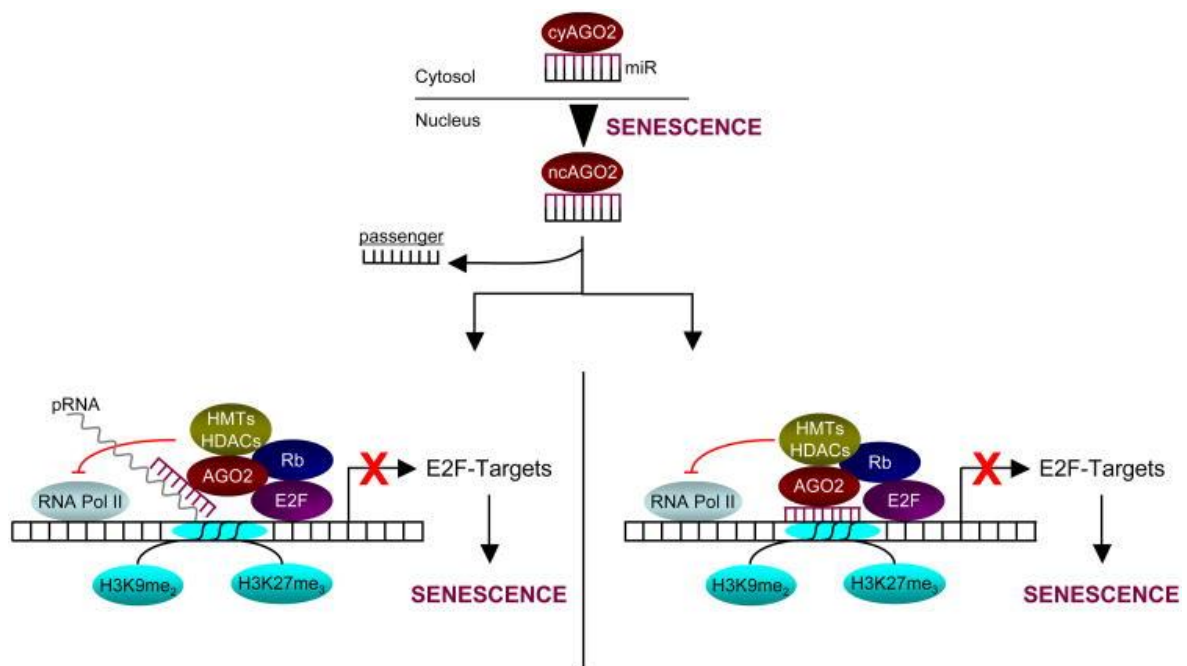


Figure 2: AGO2-mediated nuclear target gene silencing of E2F leading to cellular senescence. Rb, *let-7*, AGO2 and other effectors work in concert to repress the E2F-gene and thus lead to the initiation of cellular senescence (Benhamed, 2012)

1.4. Extracellular circulating micro-RNAs as means of communication

Since the discovery of micro-RNAs in human peripheral blood (Hunter, 2008), the question has arisen if micro-RNAs are able to act as a means of communication between cells, and if so, how cells manage to secrete these regulatory nucleic acids and protect them from RNase degradation and other harsh conditions. Cells have found a convenient way to enable long-distance intercellular communication by packing proteins, hormones and nucleic acids into a bilayer lipid membrane and excreting them into the environment. These enclosed spherical membranes are called extracellular vesicles (EVs) and are subdivided into three classes, depending on their size, biogenesis and cellular origin:

Table 1: Characterization of EVs based on their size, biogenesis and origin (György, 2011)

	Exosomes	Microvesicles	Apoptotic bodies
Size range	50 – 100 nm	100 – 1000 nm	1 - 5 μ m
Biogenesis	By exocytosis of MVBs	By budding/blebbing of plasma membrane	By release of blebs of apoptotic cells
Isolation	Differential centrifugation, sucrose gradient ultracentrifugation	Differential centrifugation	Co-culture with apoptotic cells
Detection	TEM, Western Blot, mass spectrometry, flow cytometry	Flow cytometry, capture based assays	Flow cytometry
Cellular source	Immune cells and tumors	Platelets, red blood cells and endothelial cells	Cell lines
Markers	Annexin V, CD63, CD81, CD9, LAMP1	Annexin V, tissue factor and cell specific markers	Annexin V, DNA content

As depicted in *Table 1*, exosomes are the smallest type of extracellular vesicles (50 – 100 nm) and form from late endosomes by exocytosis of multivesicular bodies (MVB). Microvesicles, being slightly larger in size (100-1000 nm), originate from the plasma membrane. Apoptotic bodies, as their name states, derive from blebs and remnants of apoptotic cells. Discrimination and selective isolation can be achieved by specific surface markers on these EVs. Being fully aware of the cell-specific origin of the EVs can help in

correct characterization as surface markers may deviate between different cell types and tissues (Yànez-Mo, 2015).

Enclosed by a lipid bilayer membrane and bound to AGO, micro-RNAs can reach a half-time of around 5 days in serum while a “naked” micro-RNA is degraded in a matter of minutes (Gantier, 2011). Hence, protein-bound and packed miRNAs could serve as robust biomarkers for both diagnostic and therapeutic approaches in modern medicine (see next chapter).

As EVs are a known communication and transportation tool between cells (Robbins & Morelli, 2014), encapsulated micro-RNAs can take part in endocrine-like signaling and reach distant parts of the body through the circulatory system. Secreted EVs are internalized by target cells either by endocytosis, membrane fusion, phagocytosis or micropinocytosis (Mulcachy, 2014). The cargo of the vesicles, including micro-RNAs, is eventually released in the cytoplasm (Kinet, 2013) and post-transcriptional regulation mechanisms, like described in the previous chapters, can now take place inside the target cell.

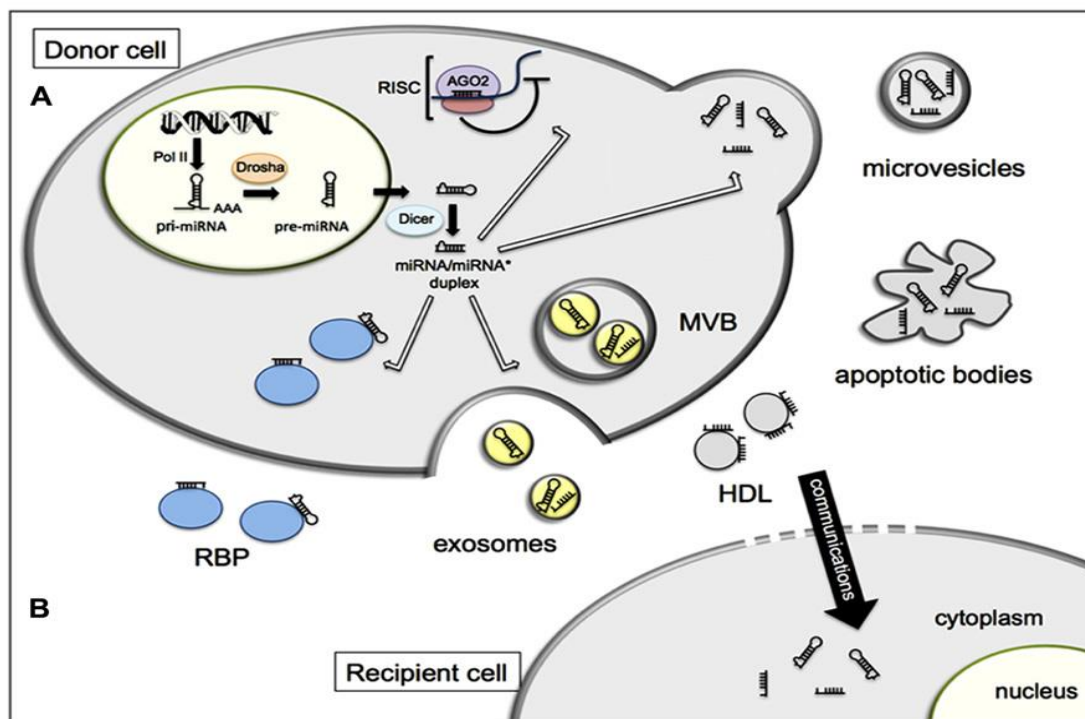


Figure 3: Packing of mature micro-RNAs into EVs, release into the extracellular space and uptake into target cells. Micro-RNAs can be either packed in EVs like apoptotic bodies, exosomes or microvesicles or are bound to proteins like HDL (high-density lipoprotein) and RBP (retinol-binding proteins), protecting them from degradation (Kinet, 2013).

1.5. Micro-RNAs as biomarkers

Micro-RNAs are not only found in serum but also in saliva, breast milk, urine, tears, seminal fluid and many others biological fluids. Due to their stability, the analysis of micro-RNAs to predict, diagnose, prognose and treat diseases has initiated an intensive study on relevance of varying micro-RNA levels in pathological and malignant outcomes.

The first indication that miRNAs play a crucial role in initiation and progress of diseases was proposed by Calin et.al. in 2002 during a study on B-cell chronic lymphocytic leukemia (BCLL). Previously, loss of a region on the chromosome 13q14 had been found to be the most frequent chromosomal abnormality in CLL (Bullrich & Croce, 2001), suggesting that the deletions at 13q14 have pathological significance. The loss of two genes within a 30-kb region caught special attention of the researchers: miR15 and miR16. They hypothesized, that both micro-RNAs play a vital role as tumor suppressors but unfortunately could not provide evidence at that time. 6 years later, Bonci et.al. provided the missing puzzle piece by discovering that the miR15 and mir16 clusters act as tumor suppressors for prostate cancer by targeting multiple oncogenic factors, especially the oncogene BCL2. Consequently, measurement of miR15 and miR16 levels in the circulatory system could predict the risk of developing oncologic pathologies linked with BCL2.

Further research in this field has led to extraordinary discoveries. Numerous micro-RNAs have been shown to be either up- or downregulated in certain pathologies – see *Table 2*. Despite the very promising discoveries so far, one has to bear in mind that pathologies like cancer rely on a knock-out or upregulation of numerous genes that usually work in concert and that a simple look on a single miRNA cannot give significant prognostic or diagnostic value. Hence, Jun Lu et.al. (2005) proposed that an expression profile with a minimum of 200 miRNAs must be established to get a glimpse on global change in miRNA expression levels (see *Figure 4*). With the help of such heatmaps, the exact taxonomy, differentiation state, and developmental lineage of tumors can be entrenched, making classification less complicated and more reliable compared to mRNA profile analysis (Lu J. , 2005).

Table 2: micro-RNAs associated with common human pathologies (Li & Kowdley, 2012)

Disease		miRNA
Cancer	B-cell-lymphoma	miR-15, miR-16
	Breast cancer	miR-125b, miR-145, miR-21, miR-155, miR-210
	Lung cancer	miR-155, let-7a
	Gastric cancer	miR-145
	Liver cancer	miR-29b
Viral diseases	HCV (Hepatitis C)	miR-122, miR-155
	HIV-1	miR-28, miR-125b, miR-150, miR-223, miR-382
	Influenza virus	miR-21, miR-223
Immune-related diseases	Multiple sclerosis	miR-145, miR-34a, miR-155, miR-326
	Systemic lupus erythematosus	miR-146a
	Type II diabetes	miR-144, miR-146a, miR-150, miR-182, miR-103, miR-107
	Nonalcoholic fatty liver disease	miR-200a, miR-200b, miR-429, miR-122, miR-451, miR-27
	Non-alcoholic steatohepatitis	miR-29c, miR-34a, miR-155, miR-200b
Neurodegenerative diseases	Parkinson's disease	miR-30b, miR-30c, miR-26a, miR-133b, miR-184*, let-7
	Alzheimer's disease	miR-29b-1, miR-29a, miR-9

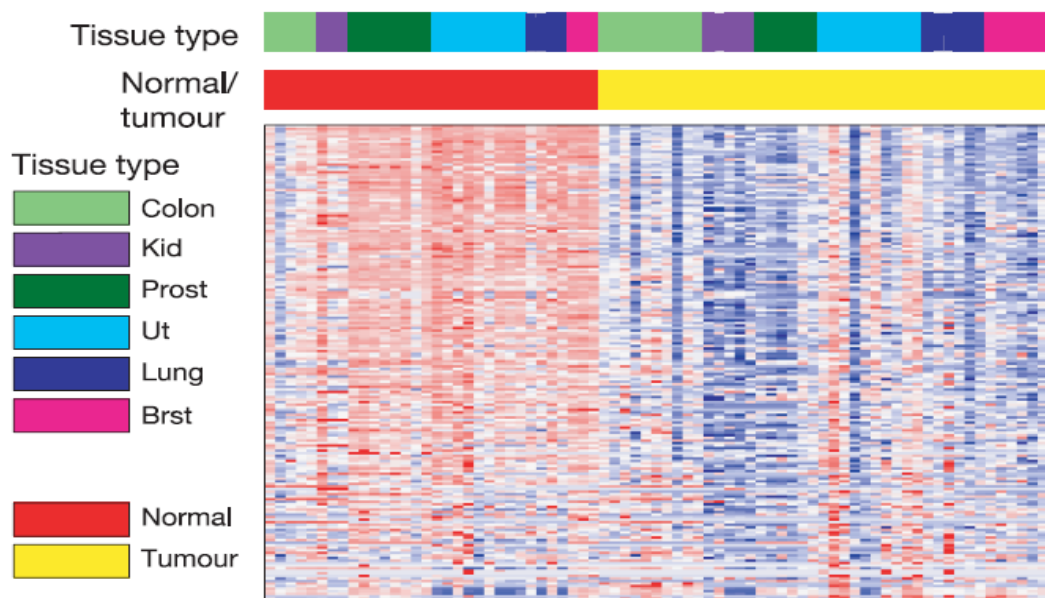


Figure 4: Heatmap of miRNA expression showing downregulation (blue color) of countless miRNAs in tumour tissue (yellow bar) compared to normal tissue (red bar) (Lu J. , 2005)

The figures and tables above show only a small glimpse of possibilities of utilizing micro-RNAs as validated biomarkers for human diseases. When it comes to routine micro-RNA biomarker analysis, RT-qPCR (real-time quantitative polymerase chain reaction) of human plasma and serum samples with micro-RNA specific primers has shown to be the most robust method. Furthermore, working with standardized methodology under RNase free environment is crucial for establishing a functional pipeline for micro-RNA quantification. Normalization to synthetic spiked-in RNA or stable reference genes and a quality control of pre-analytical and analytical variables are essential steps while setting up such assays and will be provided in this thesis and in detail discussed in the *Material and Methods* section.

1.5.1. Difference between human blood and serum

Depending on sample type, the amount and type of detectable micro-RNAs may vary, as shown by Wang, et.al. in 2012. For example, human plasma and serum differ significantly regarding composition and concentration of specific miRNA analytes. Taking a detailed look at the different way of preparation of these two matrixes reveals the reason behind it:

Serum is prepared by centrifugation of clotted whole blood and acquiring the resulting supernatant containing electrolytes, antibodies, antigens, hormones and other proteins like albumin. The main distinction to plasma is that latter is treated with an anticoagulant (e.g. heparin or EDTA) prior to centrifugation, preventing blood clotting and the release of stress factors. Consequently, plasma consists of fibrinogen and other important coagulation factors which are absent in serum but does lack important factors which are released during the coagulation process by platelets – like platelet specific micro-RNAs (Wang, 2012).

1.5.2. How to determine the hemolytic effect in blood samples?

Aside from that, the blood sampling process per se must be carefully performed and monitored. Hemolysis (rupture and lysis of red blood cells) leads to the release of cytoplasmatic content of erythrocytes affecting the total miRNA concentration and composition.

To monitor this phenomenon and correlate the obtained analytical qPCR data with this effect, researchers like Blondan, et.al. have assessed miRNA profile quality in serum and plasma by studying hemolytic samples.

A simple method to evaluate if a sample is hemolytic, is just by looking at it: The released free hemoglobin colors the sample in red and gives a good indication of hemolysis but does not reveal the progression of it. However, measuring the oxy-hemoglobin absorbance at $\lambda = 414$ nm in a spectrophotometer gives a better insight on the progress of the hemolytic effect and can help in disqualifying samples before taking time-consuming and expensive downstream analytical steps. Another way of evaluating this effect is by comparing the quantification cycle values of two distinct miRNAs with each other and establishing a so-called *hemolysis coefficient*:

$$\Delta Cq_h = Cq(miR23) - Cq(miR451) \quad (1)$$

The higher the delta-Cq, the higher the hemolytic effect. The theory behind this formula is that a specific miRNA, miR-451, has been shown to be enriched in erythrocytes as it is required in erythroid homeostasis (Rasmussen, 2010), while miR-23 is relatively stable in both plasma and serum samples, regardless of hemolysis state. Therefore, the ratio between these two miRNAs can be utilized to show the level of hemolysis. A delta-Cq above 5 gives a good hint of erythrocyte contamination while a value above 7-8 classifies the sample as an outlier and in consequence tags the specimen for disqualification (Blondal, 2013).

1.6. Introducing a special family of micro-RNAs: oncomiRs

To get an insight on the mode of action and the differences between distinct micro-RNA species, the next chapter is focused on how micro-RNAs can alter and regulate signal pathways ubiquitously. Three different so-called *oncomiRs* will be described in detail. As the name already suggests, these micro-RNAs are closely associated with oncologic diseases as their levels are either decreased or increased in cancerous tissue. Special emphasis with attention to detail is put on miR-21.

1.6.1. miR-17~92 polycistron

As reviewed by Concepcion et al, the miR-17~92 polycistron on chromosome 13, consisting of six distinct micro-RNAs (miR-17, miR-18a, miR-19a, miR-20a, miR-19b-1 and miR-92a), has been found to play a crucial role in regulation of apoptosis in diffuse B-cell lymphomas. In strong interplay with c-Myc (a cell proliferation activating gene), the members of the miR-17~92 family can suppress apoptosis and also inhibit several cell cycle arrest checkpoint proteins. Consequently, miR-17~92 is termed a *bona fide* oncogene (He & Thomson, 2005).

These first studies of Concepcion and colleagues led to several astonishing discoveries and further proof of the tumorigenic potential of miR-17~92, especially after investigating loss-of-function and gain-of-function in the E μ -Myc mouse model of B-cell lymphoma: Genetic knockout of miR-17~92 showed increased cell-death and reduced tumorigenicity while overexpression led to enhanced tumor formation potential and even improved tumor maintenance making the miR-17~92 cluster a therapeutic target in treating B-cell lymphoma (Mu & Han, 2009).

Another tumor engraftment study in C57BL6/NCr mice revealed that upregulation of miR-17~92 by Myc increases tumorigenicity by promoting angiogenesis, a process that attracts blood vessel sprouting into the tumor, which is an essential prerequisite for tumor growth and survival. This process is mediated by the repression of anti-angiogenic factors thrombospondin-1 (TSP-1) and connective tissue growth factor (CTGF) by miR-18 and miR-19, respectively (Dews, 2006). This discovery by Dews and colleagues supported the hypothesis, that expression of this cluster not only increases tumorigenicity but also is essential for tumor maintenance. A gene therapy eliminating this cluster could be a silver bullet in the fight against B-cell lymphoma.

To get a clearer overview on how this cluster can decide the fate of the cell (growth arrest vs. unlimited/tumorigenic growth), a representative picture of miR-17~92 targets is shown in *Figure 5*.

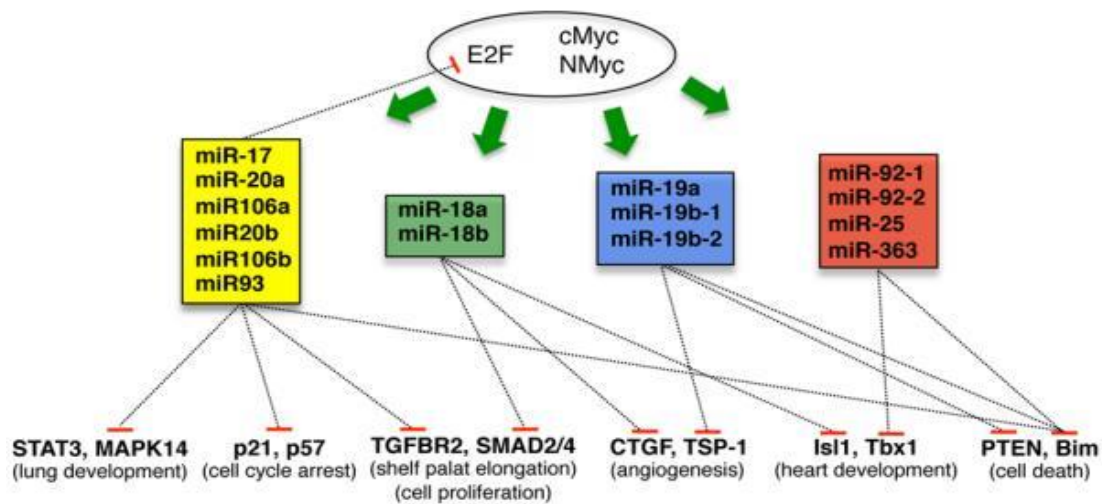


Figure 5: Schematic representation of targets regulated by miR-17~92 and paralogs. In strong cooperation with E2F and Myc, miR-17 suppresses downstream targets like PTEN and p21, which function as checkpoints in the cell cycle. This consequently promotes tumor formation. Inhibition of anti-angiogenic factors like CTGF and TSP-1 by miR-18 and miR-19, and increases tumor maintenance and survival (Concepcion, 2012)

1.6.2. miR-155

Another recently discovered key player in various physiological and pathological processes is the multifunctional micro-RNA 155, encoded by *BIC* on chromosome 21. This specific miRNA is found to be important in regulating innate and adaptive immune responses by mediating B-cell-, T-cell- and macrophage differentiation and stimulation. Figure 6 gives an overview of these two compartments of the immune system and highlights the overlapping sections. The complement pathways and cytokines are not included in this descriptive figure.

As the name suggests, the innate immune response is the first line of defense of the human body since birth, consisting of physical barriers like the skin, mucosa and cells including macrophages, granulocytes and dendritic cells. These cells possess toll-like receptors (TLRs) on their surface and identify invading organisms by recognition of pathogen-associated molecular patterns (PAMPs) like bacterial lipopolysaccharides or viral dsRNA. Once identified, they can either phagocytize invaders or label them for elimination by the adaptive immune system (Takeda & Shizuo, 2005).

On the other hand, the key players of the adaptive immune system consist of the B-cell lymphocytes and their products (so-called antibodies) and T-cell lymphocytes and their

subclasses, the T-helper and T-killer cells. The adaptive immune response is characterized by a slower reaction but higher specificity and can be divided into two groups: The *cell-mediated* response (activation of B- and T-cells) and *antibody-mediated* response (immunoglobulins secreted by B-cells). Both responses may target antigens (e.g. viral membrane proteins) and mark them for elimination by specific phagocytotic cells (Alberts, Johnson, & Lewis, 2002).

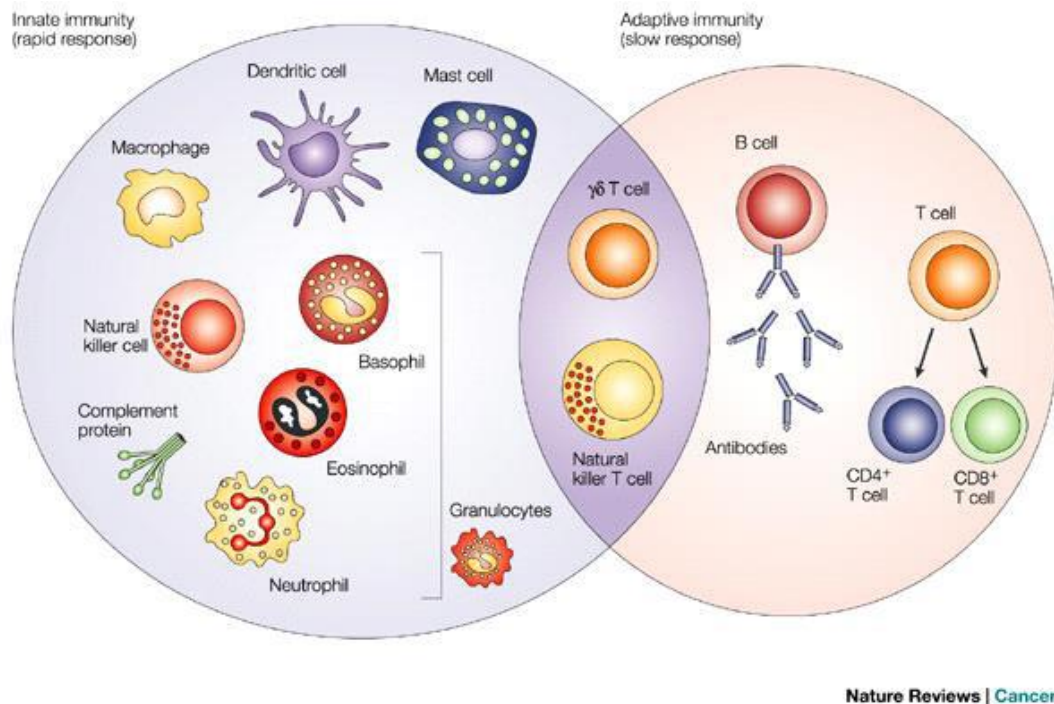


Figure 6: Comparison between the innate immune response and the adaptive immune response and the major key players of each compartment. The innate immune system comprises of granulocytes, dendritic cells and macrophages while the adaptive immune response system consists of B-cells (which secrete antibodies) and T-cells (which can either differentiate into T-helper cells (CD4+) or cytotoxic T-cells (CD8+)) (Dranoff, 2014)

As shown in Figure 7, miR-155 exhibits an important regulatory function and can interact with key players of both adaptive and innate immune response. It is especially important in the rapid inflammation response by macrophages. After recognition of PAMPs by TLRs on macrophages (e.g. LPS by TLR4), the NF- κ B pathway is set in motion which in consequence leads to activation of proinflammatory cytokine and Type I interferon genes (Lu, Yeh, & Ohashi, 2008). In the next step of this signaling cascade, TNF- α (tumor necrose factor alpha) induces expression of miR-155 which eventually causes a strong inflammatory response as it acts as a positive-feedback regulator. This feedback-loop is

caused by downregulation of downstream anti-inflammatory genes like polyphosphatase-5-phosphatase (INPP5K) and suppressor of cytokine signaling 1 (SOCS1) by miR-155 and leads to cell growth, migration and anti-pathogen response (Wang P. , 2010). Accordingly, miR-155 functions both as an anti-pathogenic mediator and biomarker of acute innate immune responses.

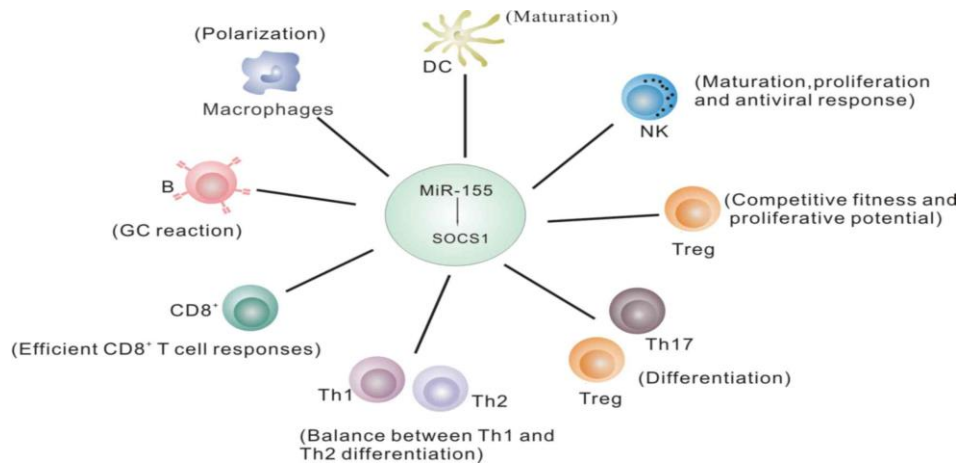


Figure 7: miR-155 affects numerous immunological mechanism on post-transcriptional level by targeting suppressor of cytokine signaling 1 (SOCS1) on post-transcriptional level (Tao, 2018) (B....B cells, Th....T-helper cells, Treg....T-regulatory cells, NK...natural killer cells, DC....dendritic cells)

The link to cancerous diseases is now formed, as it is known that the tumor microenvironment exploits the innate immune system to generate a persistent inflammatory state, promoting proliferation, survival and migration of tumor cells (Coussens & Werb, 2002). As miR-155 is overexpressed in activated macrophages and, according to publications, also upregulated in triple negative breast cancer (Jang, 2017) and B-cell lymphoma (Eis & Tam, 2005), this micro-RNA can also be exploited as therapeutic agent or prognostic marker for diseases associated with chronic inflammatory conditions (e.g. cancer or rheumatoid arthritis).

1.6.3. miR-21

As one of the most highly expressed human miRNAs and belonging to the previously mentioned group of oncomiRs, mir-21 has been extensively studied over the last years. It is encoded by the *MIR21* gene on chromosome 17 and is transcribed as a single precursor which results in a single mature miRNA after nuclear export and cytosolic cleavage as opposed to micro-RNAs derived from clusters (Kumarswamy, Volkmann, & Thum, 2011). The mature hair-pin structure can be studied in *Figure 8*.

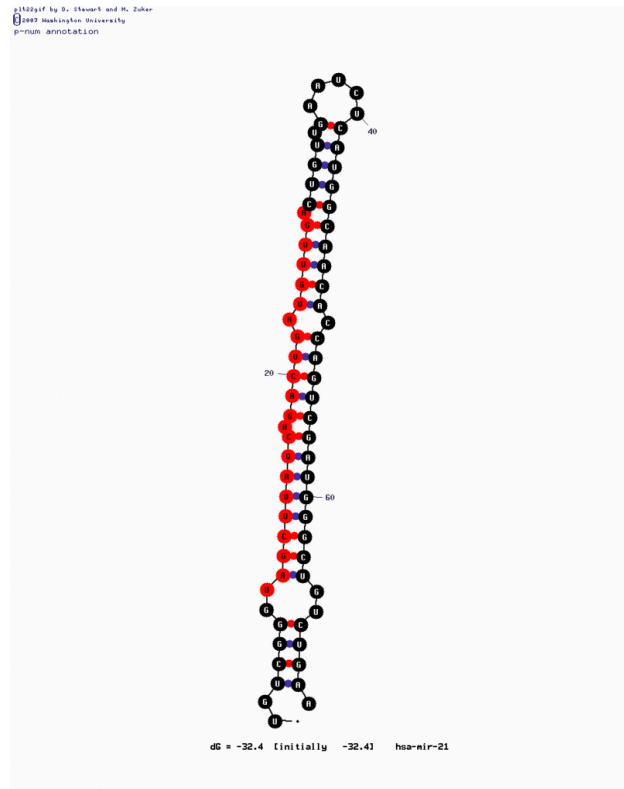


Figure 8: mature hsa-mir21. The characteristic hair-pin structure can also be seen in this figure ((c) Washington University, 2007)

As stated before, the expression of numerous micro-RNAs is deregulated in neoplastic tissues. Since some of these (classified as oncogenic micro-RNAs or oncomiRs) specifically target tumor suppressors, this leads to a non-regulated, uncontrollable growth of tumor tissue. In line with the other oncoMiRs, miR-21 is not an exception and has been found to target and downregulate several tumor suppressor genes like *PTEN* (phosphatase and tensin homolog) (Meng, et al., 2007) or *PDCD4* (programmed cell death protein 4) (Asangani, 2007) resulting in increased tumorigenic and metastatic potential.

1.6.3.1. PI3K-Akt pathway

In healthy cells, *PTEN*, a direct target of miR-21, plays a pivotal role in the PI3K-Akt pathway by dampening the strength of this signaling cascade, consequently regulating apoptosis and cell cycle arrest. If these regulatory mechanisms are disrupted either by mutation or targeted downregulation of *PTEN*, the cell cycle may continue endlessly and without

control. Therefore, affected cells continue to duplicate without a stop-signal (apoptosis or cell cycle arrest) while also accumulating DNA damage and mutations, eventually leading to cancerous growth. It is not a coincidence that PTEN mutations can be detected in at least 20% of glioblastomas (Wang, Puc, & Li, 1997), even being the most frequently mutated gene in prostatic cancer (Cairns, Okami, & Halachmi, 1997), rivaling p53 in mutation frequency in sporadic oncologic diseases. Looking at the PI3K/Akt pathway and its network of components can help to understand how loosening of a single screw can affect the whole signal machinery, emphasizing how fragile such important pathways can be (Figure 9).

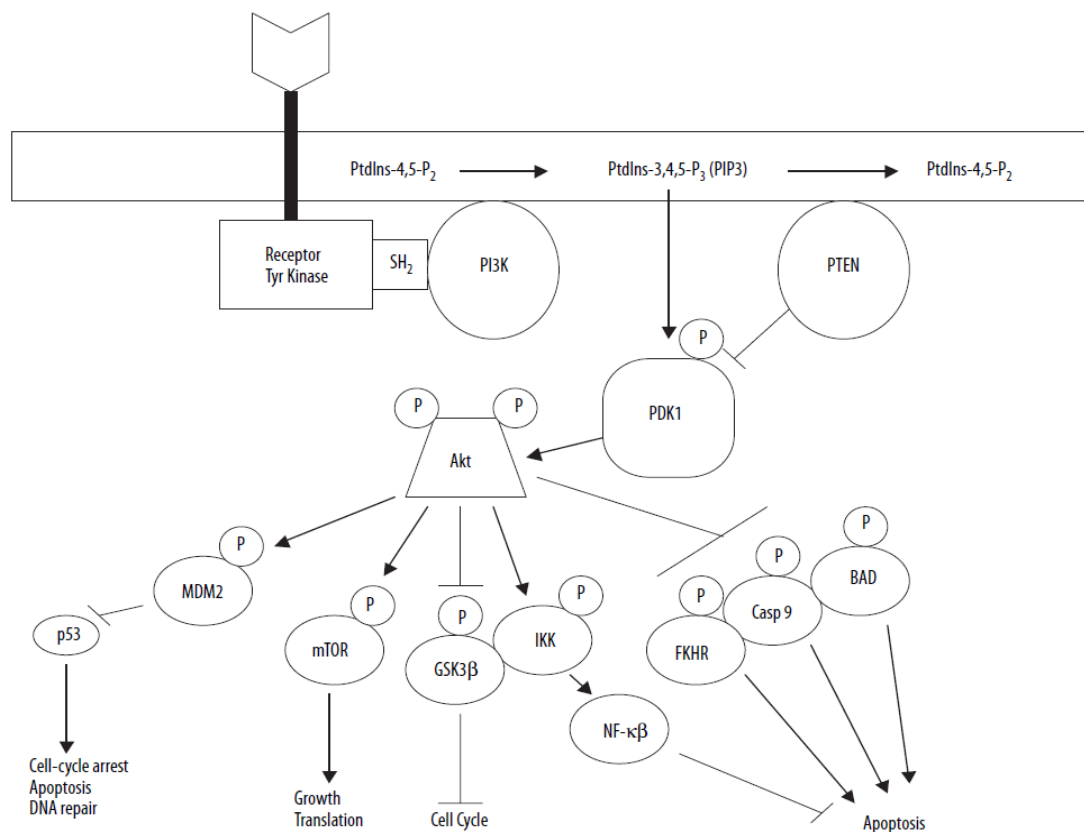


Figure 9: Overview of the PI3K-Akt pathway: After binding of growth hormones like EGF or IGF-1 to the receptor tyrosine kinase, the signaling cascade is kindled, leading to the activation of Akt via PI3K and PDK1. In following, Akt activates downstream targets which trigger expression of growth stimulating genes like mTOR and inhibition of apoptosis inducing genes like p53 and Caspase 9. Activated PTEN acts as a lagged disruptor and suppressor of Akt by dephosphorylation of PIP3 and further decrease of Akt activity. (Chu & Tarnawski, 2004)

After activation of the receptor tyrosine kinase on the outer membrane of the cell through binding partners like f.eg. insulin, the intracellular domains of the receptor dimerize and auto-phosphorylate, leading to activation of PI3K. PI3K then catalyzes the conversion of

phosphatidylinositol (3,4)-bisphosphate (PIP2) to phosphatidylinositol (3,4,5)-trisphosphate (PIP3). Here, PTEN, comes into play: as a lipid phosphatase, it acts as the antagonist of PI3K by dephosphorylating PIP3 to generate PIP2. Hence, it functions as a time-regulated checkpoint, preventing hyperstimulation of the PI3K-Akt pathway.

After PIP3 synthesis, PIP3 dependent kinase 1 (PDK1) is activated and eventually phosphorylates Akt, which further phosphorylates target proteins like BAD, mTOR, MDM2 and CASP9. Those in turn can then promote protein synthesis and cellular proliferation while inhibiting apoptosis and cell-cycle arrest on a genome-wide level (Chu & Tarnawski, 2004).

Consequently, post-transcriptional inhibition of PTEN by miR-21 leads to an overflowing stimulus of the PI3K-Akt pathway promoting cellular growth and disabling cell cycle control functions. Studies showed, that miR-21 has been found to be elevated in cisplatin resistant cells (Yang, et al., 2013), again indicating that apoptosis is hindered due to regulation of PTEN via miR-21. Additionally, this study also noticed that downregulation of miR-21 can reverse this apoptotic resistance, making a combinational treatment with cisplatin and miR-21 suppression a viable option for chemotherapy.

1.7. Milk – only nutritional or also functional value?

In recent years, while discovering the regulatory functions of micro-RNAs and evaluating the oncogenic potential of these non-coding RNAs, researchers also tried to identify a functional value in consumer products. Especially dairy products, more precisely milk, generated a lot of research interest, since it is essential for delivering important nutrients to the mammalian offspring. With 4% protein, 3% fat, and 20% carbohydrate content, milk delivers an essential amount of energy to both infant and adolescent mammals, which is needed to keep the metabolism and growth of the body in motion. Moreover, the process of lactation distinguishes mammals from other species and may be at least partially responsible for the rise of the mammalian species to the peak of the food chain.

Taking this information into account, the common hypothesis of the scientific world states that the process of lactation and consumption of maternal derived milk must also improve

the overall health of the offspring and give an edge over predatory species. With the identification of immune-related micro-RNAs in breast milk exosomes (Zhou & Li, 2012), a milestone in evaluating the functional value of milk has been set.

Nowadays, two hypotheses about the impact of milk miRNAs on human health exist, as described by Melnik (2016):

- the *functional hypothesis*, which elaborates that the transfer into the systemic circulation and subsequent function of milk mRNAs in the offspring are valid mechanisms which lead to genetic regulation in the recipient.
- and the *nutritional hypothesis*, which states that both exosomes and packed micro-RNAs are degraded in the intestinal lumen for nutritional purposes only and have therefore no specific regulatory effect.

Additionally, a third hypothesis exist, which hybridizes both theories above into one: an *age-dependent functional hypothesis*.

Studies showed, that the intestinal permeability varies depending on age and health. Especially during postnatal and infant age, the intestinal barrier has been found to be more permeable to particles like exosomes (Macierzanka, et al., 2014). Hence, in the postnatal phase, where the offspring is highly dependent on immunological and growth stimuli, milk micro-RNAs could play a pivotal role in development. In contrast, in the adolescent phase, excessive growth stimuli should be avoided due to the increased risk of developing sporadic neoplastic. This could be circumvented by enforcing the intestinal barrier with age, making it impassable for packed regulatory miRNAs.

2. Aim

Reviewers pointed out the possibility of an immunomodulatory effect in infants after uptake of milk miRNAs during breastfeed (Alsaweed, 2015). Additionally, evidence has been provided that cow milk contains high amounts of micro-RNAs (Kirchner, 2016), hence supporting the hypothesis that the contents of milk might not just simply be of nutritional but also of regulatory value.

With the premise of packed micro-RNAs being able to survive simulated gastrointestinal tract conditions (Benmoussa, 2016), we want to show in this master thesis a transfer of dietary cow-milk miRNA through the intestinal barrier into the blood stream of genetically modified mice. To narrow down micro-RNA candidates, we have put our focus on an oncogenic micro-RNA, miR-21. This decision is based on one hand on the hypothesis, that milk is important in infant growth stimulation and may therefore contain an increased amount of onco-miRs. On the other hand, the research group has access to miR-21 knock-out mice, which are ideal candidates to see even slight increases in miR-21 content due to their genetic background.

In a pilot study, we first plan to evaluate the amount of miR-21 in pasteurized and UHT treated milk with state-of-the-art methods like highly sensitive miRNA-specific qPCR. Then, a feeding scheme for the mice will be designed, including removal of blood at different timepoints throughout the experiment. At the end of the experiment, animals will be sacrificed and organs will be harvested for additional evaluation of miR-21 levels in mouse tissue.

Depending on the result of our study, we hope to bring more insight into the uptake mechanisms of dietary micro-RNAs.

3. Material and Methods

All experiments and methods were conducted in accordance to good laboratory practice (GLP) and recorded in a lab book provided by the University of Natural Resources and Life Sciences Vienna. If not otherwise stated, the experiments were performed at room temperature and under aseptic conditions.

The experiments with the mouse model organism were carried out according to the regulations of FELASA and the Ethics Committee for the Care and Use of Laboratory Animals at the Medical University Vienna (Vienna, Austria).

3.1. Materials

3.1.1. Disposables

Table 3: Disposables

Material	Manufacturer
Pipette tips (1000 µl, 200 µl)	Greiner Bio-One, Kremsmünster (A)
Pipette tips (10 µl)	Starlab, Hamburg (D)
Micro tubes, 1.5 ml, sterile	Sarstedt, Nürnbergrecht (D)
Cryotube vials 2.0 ml, sterile	Thermo Scientific, Waltham (USA)
Falcon centrifuge tubes, 15 ml, 50 ml	Corning, Corning (USA)
Micro tubes, 2.0 ml, sterile	Sarstedt, Nürnbergrecht (D)
BD Vacutainer blood collection tube with lithium heparin, 3 ml	Thermo Scientific, Waltham (USA)
Rotorgene 4-strip tubes, 0.1 ml	Starlab, Hamburg (D)
PCR-tubes, 8-tube strips, 0.2 ml	Biozym, Vienna (A)
RNeasy® Mini spin column 2.0 ml	Qiagen, Hilden (D)
QIAshredder homogenization column 2.0 ml	Qiagen, Hilden (D)
Surgical disposable scalpels	B Braun, Maria Enzersdorf (A)
RNase Zap wipes	Ambion, Carlsbad (USA)
Gloves, semperguard® nitrile	Semperit, Vienna (A)
Gloves, Semper Care Premium	Semperit, Vienna (A)

3.1.2. Equipment

Table 4: Laboratory equipment used

Equipment	Model	Manufacturer
Pipettes	Research Plus, 100 - 1000 μ l	Eppendorf, Hamburg (D)
	Research Plus, 20 - 200 μ l	Eppendorf, Hamburg (D)
	Research Plus, 2 - 20 μ l	Eppendorf, Hamburg (D)
	Research, 0.5 - 10 μ l	Eppendorf, Hamburg (D)
	Research, 0.1 - 2 μ l	Eppendorf, Hamburg (D)
	Pipetman, 100 - 1000 μ l	Gilson, Middleton (USA)
	Pipetman, 20 - 200 μ l	Gilson, Middleton (USA)
	Pipetman, 10 - 100 μ l	Gilson, Middleton (USA)
	Pipetman, 2 - 20 μ l	Gilson, Middleton (USA)
	Pipetman, 0.1 - 2 μ l	Gilson, Middleton (USA)
Laminar hood	HBB 2448 LaminAir	Holten, Hanau (D)
PCR cycler	Biometra Trio Thermocycler	Biometra, Göttingen (D)
RT-qPCR cycler	Rotorgene GenQ 6000	Qiagen, Hilden (D)
Centrifuge	Centrifuge 5415 R	Eppendorf, Hamburg (D)
	Centrifuge 5810 R	Eppendorf, Hamburg (D)
	Centrifuge 5804 R	Eppendorf, Hamburg (D)
Vortex mixer	VF2	IKA, Staufen (D)
Spectroscope	NanoDrop OneC UV/VIS	Thermo Scientific, Waltham (USA)

3.1.3. Chemicals

All chemicals and reagents were provided by Qiagen (Hilden, D), AppliChem (Darmstadt, D), Merck (Darmstadt, D), Thermo Scientific (Waltham, USA) and Sigma-Aldrich (Neu-Ulm, D). Exact description and usage of these chemicals for the respective experiments are stated in the *Methods* section of this chapter.

The used milk for this experiment was regular cow milk from Milfina bought at a local store (Hofer KG). The two variants included:

- UHT treated milk (Haltbare Vollmilch 3,5%, Milfina, stored at room temperature)
- Pasteurized milk (Vollmilch 3,5%, Milfina, stored at 4°C)

3.1.4. Primers

All primers for the micro-RNA targets and synthetic control spike-ins were provided and validated by Qiagen (Hilden, D). Due to commercial reasons, the primer sequences are confidential in nature. In the following table, the used primers with their respective target sequences are represented.

Table 5: Used sequences for miRCURY LNA™ qPCR assay

Primer	Cat. Nr.	Target sequence
hsa-miR-17-5p, miRCURY LNA™ miRNA primer assay	YP02119304	CAAAGUGCUUACAGUGCAGGUAG
hsa-miR-21-5p, miRCURY LNA™ miRNA primer assay	YP00204230	UAGCUUAUCAGACUGAUGUUGA
U6 snRNA (hsa, mmu), miRCURY LNA™ miRNA primer assay	YP00203907	GUGCUCGCUUCGGCAGCACAUUACUA AAAUUGGAACGAUACAGAGAAGAUU AGCAUGGCCCCUGCGCAAGGAUGA CACGCAAUUCGUGAAGCGUCCAUAUUUUU
UniSp2, miRCURY LNA™ miRNA primer assay	YP00203950	Unknown
UniSp4, miRCURY LNA™ miRNA primer assay	YP00203953	Unknown
UniSp6, miRCURY LNA™ miRNA primer assay	YP00203954	Unknown

3.2. Methods

3.2.1. Mouse breed

Five healthy, adult, male C57BL/6 mice (7 months old) were provided by Jackson Labs (Bar Harbor, USA). The mice had different genetic makeups, with two mice being a full knockout (**ko**) of miR-21, two heterozygotes (**het**) and one wildtype (**wt**). The knockout strain was developed as follows (taken from Jackson Lab homepage, 18/04/19): *To delete the miR-21 locus within the miR-21~Tmem49 transcriptional unit, a targeting vector was designed to replace the 93 bp precursor to miR-21 (pre-miR-21) sequence with a pGK-gb2 loxP/FRT-flanked neomycin resistance cassette.*

The construct was electroporated into (C57BL/6N x 129S6/SvEvTac)F1-derived "iTL1 BA1" embryonic stem (ES) cells. Correctly targeted ES cells were injected into recipient blastocysts and chimeric mice were bred with C57BL/6 mice (unknown substrain) to establish the colony. Mice homozygous for the miR-21-null allele (on a mixed C57BL/6;129S6/SvEv genetic background) were bred together for several generations prior to sending to The Jackson Laboratory Repository. Upon arrival, mice were bred to C57BL/6NJ (Stock No. 005304) for at least one generation to establish the colony. Heterozygous mice were generated by crossing wildtype with miR-21 ko.

Table 6: Overview of provided mice and their genotype

Strain: MIR21KO (JAX stock #016856)			
Full line: MIR21KO m2(B6) 31CA 2BC 1IC m26 m44 m6			
Name	ID BOKU	ID Jackson Lab	Genotype miR-21
Mouse 1	30	GGRI-12304	-/-
Mouse 2	34	GGRI-12308	+/+
Mouse 3	33	GGRI-12307	+/-
Mouse 4	32	GGRI-12306	-/-
Mouse 5	31	GGRI-12305	+/-
Date of birth	25/02/18		
Begin experiment	14/09/18		
Date of death	27/09/18		

3.2.2. Mouse feed and experimental timeline

Table 7: Timeline of the experiment including task and objective listing

Start Date:	18.09.2018														
TASK	Week 1							Week 2							OBJECTIVE
	mo	tu	we	th	fr	sa	su	mo	tu	we	th	fr	sa	su	
	18	19	20	21	22	23	24	25	26	27	28	29	30	1	
1st blood sample [60 µl] - serum															Genotype determination
UHT-milk feed															Feed of miRNA-free milk
2nd blood sample [60 µl]- plasma															Timepoint 1 for analysis
water feed															Wash out of possible miRNAs
3rd blood sample [60 µl] - plasma															Timepoint 2 for analysis
pasteurized milk feed															Feed of miRNA-containing milk
final blood sample [60 µl] - plasma															Timepoint 3 for analysis
death of mice and organ harvest															Determination of final miRNA concentration
lab analysis															qPCR, data normalization and interpretation

The mouse experiments including keeping, feeding and termination were conducted at the mouse keeping facility at the Institute for Cancer Research of the Medical University of Vienna.

The feeding scheme, as depicted in *Table 6*, began with 3 days of UHT-milk feed followed by 3 days of water feed and was concluded with 3 days of pasteurized milk feed. The mice were kept in the same cage at room temperature and the drinking bottle was simply filled with the respective milk variant or water. The health and weight of the mice were checked daily. In order to determine a potential intake of milk miRNA into the murine bloodstream, 60 µl of mouse blood from the mandibular vein was collected and further processed (see 3.2.4.). The termination of the mouse experiment including organ harvest was performed on 27/09/18.

3.2.3. Mouse organ harvest

After termination of the mice, the organs were harvested with a scalpel and a tweezer. The isolated organs were immediately transferred into a labelled cryotube and frozen in liquid nitrogen (-196°C) to avoid any autolysis or (mi-)RNA degradation. Long-term storage of organs was conducted at -80°C.

Following organs were isolated from each mouse:

- **Liver**
- **Small intestine** (flushed with ddH₂O)
- Inguinal lymph nodes
- Spleen
- Kidney

The liver and small intestine were further processed for analytical purposes (RNA extraction, qPCR).

3.2.4. Murine blood preparation

The blood collection of mouse specimen was performed through the mandibular vein at the beginning of the experiment and at each day of feed change to monitor any changes in systemic micro-RNA concentration. The first blood samples on day 1 of the experiment were serum in nature and used for genotyping. The blood was collected in 1.5 ml Sarstedt tubes and after 30 minutes of incubation at room temperature (blood clotting process), the samples were centrifuged for 10 minutes at 1000 g. The supernatant/serum was carefully aspirated and transferred into a new Sarstedt 1.5 ml tube and stored at -80°C until further processing.

For the following blood samples (timepoints 1-3) the decision was made to change to heparin plasma due to higher yields in volume. Therefore, the collected blood was transferred into heparin coated collection tubes and centrifuged for 10 minutes at 1000 g. The supernatant/plasma was pipetted into a Sarstedt 1.5 ml tube and stored at -80°C.

For both plasma and serum, an aliquot of 60 µl was used for further processing.

3.2.5. RNA-isolation from biofluids (serum, plasma, milk)

RNA isolation from biofluids (serum, plasma, milk) was performed according to both TAmiRNA SOP and the Qiagen miRNeasy Mini Kit (Qiagen, Cat: 203203) protocol and is based on phenol-guanidine lysis of samples with silica-membrane-based purification of total RNA. The used lysis reagent (TRIzol LS, Thermo Fischer Scientific, Cat: 10296010) is a monophasic solution of phenol and guanidine thiocyanate, designed to facilitate lysis of tissues, inhibits RNases, and removes most of the cellular DNA and proteins from the lysate by organic extraction.

200 µl of thawed plasma/serum/milk was transferred into a 1.5 ml tube (200 µl milk; 60 µl plasma/serum + 140 µl NFW, nuclease free water). To each sample, 1000 µl of lysis mastermix was added: 1000 µl TRIzol * (n + 0.05) + 1 µl RNA-Spike-In mix Usp2,4,5 (Qiagen, Cat: 339390) * (n + 0.05); n = number of samples. The lysis reaction was mixed by pipetting up and down 10 times, then samples were vortexed for 10 seconds and incubated for 10 minutes at RT. 200 µl of chloroform (Sigma Aldrich, Cat: C2432) was added to each tube and after 10 seconds of vortexing and 3 minutes of incubation at RT, the samples were centrifuged for 15' at 4°C, 12000 g. 650 µl of aqueous phase was transferred into a new 2.0 ml tube. 7.0 µl of concentrated glycogen (Invitrogen, Cat: AM9510) was added and after vortexing, 975 µl (1.5 volumes) of 100% ethanol was supplemented. The tubes were inverted 5 times and 700 µl of the mix was transferred to a RNeasy Mini Spin Column. Total RNA was bound to the column by spinning for 30 seconds at RT, 12000 g. This step was repeated with the residual volume until all of the sample was loaded onto the column – the flow-through was discarded. In the next step, the column was washed by addition of 1 x 700 µl RWT (Qiagen) and 3 x 500 µl RPE (Qiagen). After each addition, the column was centrifuged for 1 min at RT, 12000g and flow-throughs were discarded. Then, the column was transferred to a new 1.5 ml tube and after addition of 30 µl NFW at the center of the column membrane and incubation for 1' at RT, total RNA was eluted for 1 min at RT, 12000 g. The RNA was stored at -80°C.

3.2.6. RNA isolation from tissue (organs)

RNA isolation from tissue was performed in similar fashion to the methods described above. Approximately, 30 mg of tissue was cut into tiny pieces with a scalpel in a laminar hood and transferred into a weighed 1.5 ml tube. The net weight of the cut tissue was noted and in the following step, 700 μ l of TRIzol LS was added. The samples were vortexed for 10 seconds and incubated for 10' at RT. Then, the sample was centrifuged for 5' at RT, 12000 g, and the supernatant was transferred into a QIAshredder column (Qiagen, Cat: 79654) for high-molecular DNA shearing and sample homogenization. After another centrifugation step for 2' at RT, 12000 g, 140 μ l chloroform was added to the homogenized flow-through. The sample was vortexed for 15 seconds, incubated for 3' at RT and centrifuged (12000 g, 15', 4°C). Next, 200 μ l of aqueous phase was transferred to a new 1.5 ml tube, where 1.5 volumes of 100% ethanol (300 μ l) were supplemented. The sample was mixed by pipetting and then loaded onto a Qiagen miRNeasy column. Washing and elution steps were performed as in 3.2.5. (biofluid RNA isolation). Total RNA was measured at Nanodrop ONE/C UV VIS based on absorbance of nucleic acids at 260 nm. Storage was conducted at -80°C.

3.2.7. Heparinase treatment of total RNA

Heparin is a known inhibitor of polymerases as it irreversibly binds to DNA interacting proteins – as such, heparin negatively affects the enzymatic reactions in qPCR and cDNA synthesis. A precautionary step would be to avoid heparin plasma at all costs, but if this is not the option, heparinase digestion is a valid alternative. In this study, heparin plasma samples were the only option to achieve a sustainable sample amount. Hence, a heparinase treatment of total RNA was performed with Heparinase I from Flavobacterium Heparinum (Sigma-Aldrich, Cat: H2519-50UN) according to manufacturer's protocol. The reaction was performed at 25°C for 3h.

Table 8: Reaction setup for heparinase digestion of total RNA

Component	Volume per rxn
Heparinase I	1.25 μ l
RiboLock RNase Inhibitor (Thermo Fischer, Cat: EO0381)	0.25 μ l
Heparinase buffer (10 mM Tris, 25 mM NaCl, 2 mM CaCl ₂ pH = 7.5)	3.5 μ l
RNA isolate	5 μ l
Total	10 μl

3.2.8. Complementary DNA (cDNA) synthesis

Single-stranded RNA was analyzed by qPCR and had to be reversely transcribed first into complementary double-stranded DNA (cDNA). For this, the miRCURY LNA™ RT Kit (Qiagen, Cat: 339340) was used according to the manufacturer's protocol. Biofluid RNA and tissue RNA were handled differently, as seen in the following tables: For biofluids a constant volume was used (2 μ l) while for tissues a defined amount of RNA was used (5 ng). To minimize RNA degradation, the pipetting steps were performed on ice.

Table 9: Reaction setup for cDNA synthesis from biofluid samples

Component	Volume per rxn
5x RT reaction buffer	2 μ l
NFW	4.5 μ l
10x RT-enzyme	1 μ l
Usp6 control	0.5 μ l
RNA template (biofluid, undiluted)	2 μ l
Total	10 μl

Table 10: Reaction setup for cDNA synthesis from tissue samples

Component	Volume per rxn
5x RT reaction buffer	2 μ l
NFW	4.5 μ l
10x RT-enzyme	1 μ l
Usp6 control	0.5 μ l
RNA template (tissue, 5 ng)	2 μ l
Total	10 μl

The reaction mix was set-up in 0.2 ml PCR tubes and transferred into the thermocycler for reverse transcription. The program was performed as followed and comprises of three steps, elongation (step 1), denaturation (step 2) and cooldown/storage (step 3).

Table 11: Cycling program for RT reaction using the miRCURY LNA™ RT kit

	Step 1	Step 2	Step 3
Temperature [°C]	42	95	4
Time [min]	60	5	∞

3.2.9. Real-time quantitative polymerase chain reaction (RT-qPCR)

Real-time qPCR is a state-of-the-art nucleic acid detection method which combines amplification and detection of nucleic acids in one step. By using DNA-binding fluorescent dyes like Sybr Green, one can detect target DNA amplification with the respective primer until the fluorescence signal exceeds a defined threshold, the so-called cycling value (Ct). The Ct value is a standardized readout and reflects how many cycles it takes until the reaction reaches a fluorescence intensity above background levels (see Figure 8).

In our experiments, we used the miRCURY LNA SYBR® Green PCR Kit (Qiagen, Cat: 339345) for sensitive and specific detection and quantification of target micro-RNAs. This kit uses a locked nucleic acids (LNA) technology, which “locks” the ribose in the ideal conformation for Watson-Crick binding. This allows for higher binding affinity and discrimination of closely related miRNA sequences.

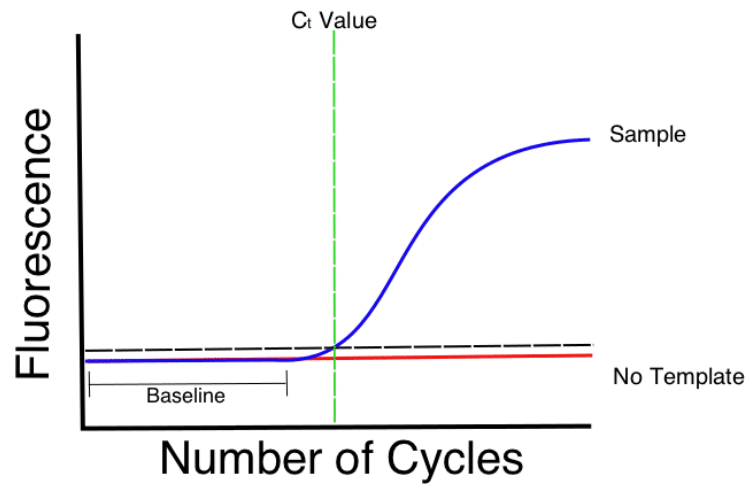


Figure 10: Determination of Ct value in a qPCR reaction: The intersection between sample fluorescence curve and defined background fluorescence threshold gives the Ct value (Oswald, 2018)

The reaction was set up according to manufacturer’s protocol (see *Table 12* and *13*) and analyzed in a Rotorgene Gene Q qPCR cyler (Qiagen) in duplicates. For both tissue and biofluid samples (serum, plasma, milk), a 1:40 cDNA dilution was used as template. The $\Delta\Delta C_t$ method was used for quantification of miRNAs and the Ct values were obtained by setting the manual threshold to 0.01. The used primers can be evaluated in the *Materials* section. As non-template-control, NFW was used instead of cDNA.

Table 12: Reaction setup for qPCR using the miRCURY LNA SYBR® Green PCR Kit

Component	Volume per rxn
2x miRCURY SYBR Green Master Mix	5 μ l
PCR primer mix (U6, miR-21,...)	1 μ l
cDNA template (1:40 dilution)	4 μ l
Total	10 μl

Normalization ($\Delta\Delta C_t$ method) of obtained Ct values was performed to reduce technical variation between samples to a minimum. For this purpose, synthetic spike-ins were added to each technical step in this experiment (Usp2 for RNA isolation and Usp6 for cDNA synthesis). For the final analysis, the Ct values were normalized to either an endogenous, stably expressed reference gene (U6 snRNA for tissue samples) or the synthetic spike-in (Usp 2 for biofluid samples) (see *Results*).

Table 13: Temperature and cycling profile for use of miRCURY LNA SYBR® Green PCR Kit

Action	Cycles	Temperature [°C]	Time [sec]	Ramp rate	Acquisition Mode	Acquisition per °C
Activation	1	95	120	Max		
Quantification (2-step-cycle)	45	95	10	Max	single	
		56	60	Max		
Melting Curve	1	56 - 90			continuous	1

3.2.10. Statistics

For statistical analysis of the obtained results, paired Student's t-test was used. A p-value below 0.05 was considered significant.

4. Results

According to literature, UHT processed milk contains less miRNAs than pasteurized milk (Kirchner, 2016). To ensure, that literature data can also be applied in our experimental setting and that we can use UHT milk as an internal “matrix” control, we decided to evaluate the miRNA levels in our milk samples (UHT and PAS) before performing animal experiments.

4.1. miR-21 quantification in pasteurized and ultra-high-temperature treated milk

In this preliminary test, we quantified the total RNA content and the circulating amount of miR-21 in both pasteurized (PAS) and UHT milk. For this experiment, 2x 200 µl of each milk sample was used. Normalization was performed according to following formula:

$$\text{normalized Ct} = Ct(Usp2) - Ct(miR21) \quad (2)$$

The obtained values can be studied in the next figure (*Figure 11*) showing a bar chart with the normalized Ct values. Due to the nature of normalization and qPCR analysis, a higher normalized Ct value equals a higher copy number of target micro-RNA. In this respective experiment, and following the assumption that one cycle in qPCR corresponds to one doubling of copy number (2^n , n = cycle number), the miR-21 concentration in pasteurized milk (Ct mean = -3.915) is roughly 217 times higher than in UHT milk (Ct mean = -11.675). Non-template runs with NFW gave no fluorescence signal.

The levels of miR-17 were also analyzed in this setup, but no signal could be detected.

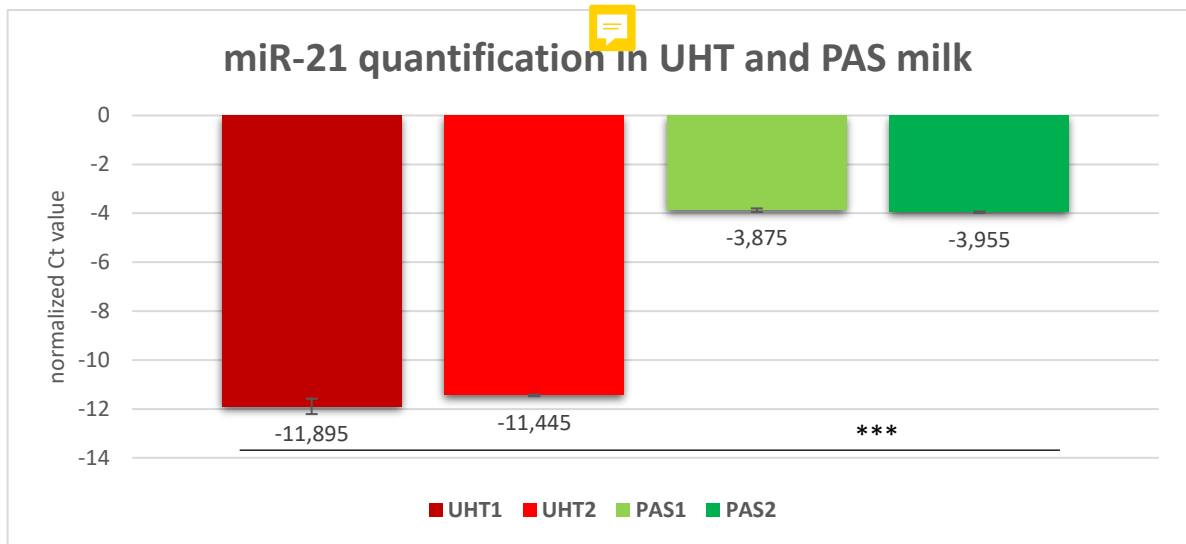


Figure 11: Normalized Ct values of each milk variant showing a higher amount of miR-21 in pasteurized milk than in UHT milk. (n=2, technical replicates, standard deviation represented in error bar, $p \leq 0.001$)

For experimental quality control, the technical variation of each preparation step was monitored by amplification of the synthetic spike-ins during quantitative PCR. As mentioned in the *Methods* section, Usp2 was used to evaluate the quality of the RNA isolation while Usp6 was added to check for aberrations during cDNA synthesis. Deviations in a single spike-in control or in both can give a hint in which technical step a technical error might have occurred. This is crucial when establishing a pipeline according to GMP standards, as significant outliers need to be either excluded or sample analysis needs to be repeated. In our experiment, no critical deviations were noticeable (see *Figure 12*).

The samples 1-4 correspond to UHT1 and UHT2 milk with each technical replicate shown as a single data point. Samples 5-8 stand for PAS1 and PAS2.

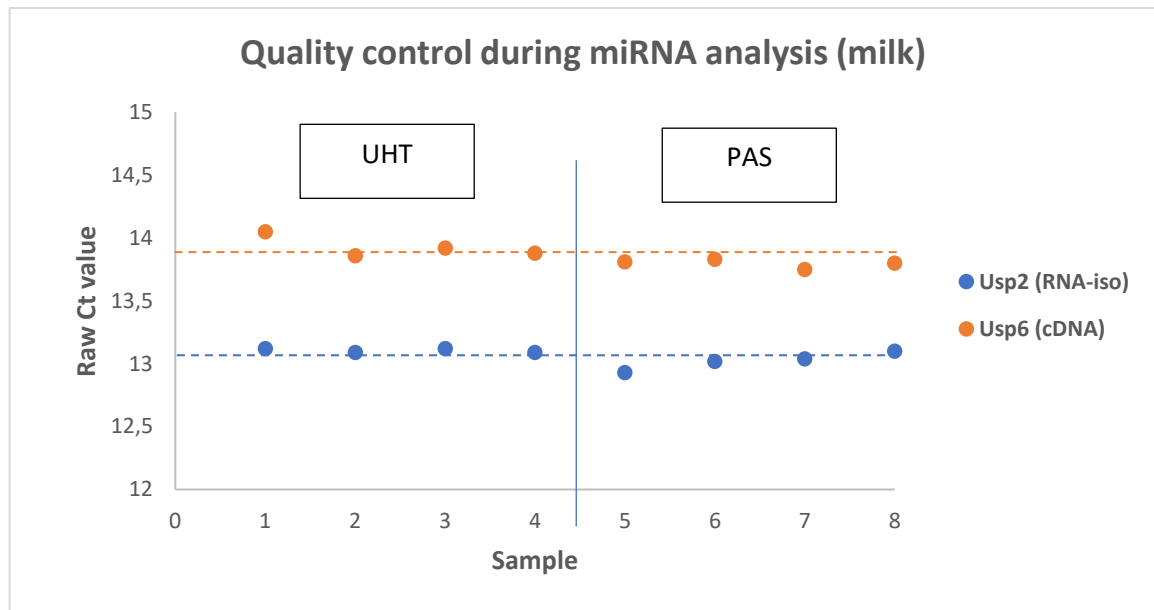


Figure 12: Evaluation of quality of RNA isolation and cDNA synthesis during milk micro-RNA analysis. Usp2 was added during RNA isolation while Usp6 was spiked in during cDNA synthesis. The dashed line represents the respective mean value of each spike in control. Each datapoint corresponds to a single technical replicate.

4.2. Mouse genotyping miR-21

Next, we verified the genotype of the ~~delivered~~ mice. Blood serum samples from each mouse were taken before the start of the animal experiment and were used to quantify miR-21 and miR-17 levels by qPCR. The corresponding data are shown as normalized values (Usp2 normalization in *Table 14*).

The miR-21 background of each mouse was confirmed and matched the data provided in the delivered genotype sheet by Jackson Labs, showing a difference of roughly 16 cycles (65536-fold) between **knockout** and **wild type** strain. The **heterozygous** miR-21 values were slightly lower (roughly two cycles, corresponding to 4-fold lower concentration). In line with our expectations, the Ct values of miR-17 were rather even between the different genetic strains, spanning from the maximum Ct of -11.89 to the minimum Ct of -15.71. As in the previous experiments, a higher Ct corresponds to a lower copy number of the analyte.

Table 14: Confirmation of miR-21 mouse genotype and comparison of miR-17 values

Mouse	Raw Ct (Usp2)	Raw Ct (miR-17)	Raw Ct (miR-21)	Normalized Ct (miR-17)	Normalized Ct (miR-21)
1 (-/-)	14.57	26.64	33.72	-12.07	-19.15
2 (+/+)	14.63	28.32	18.36	-13.69	-3.73
3 (+/-)	14.61	30.32	21.08	-15.71	-6.47
4 (-/-)	14.51	28.23	34.68	-13.72	-20.17
5 (+/-)	15.00	26.89	19.37	-11.89	-4.37

The quality of the samples was again checked with the help of the synthetic spike ins, showing no outliers or technical errors. Each mouse blood sample was analyzed in technical duplicates (qPCR) and is represented as a single data point.

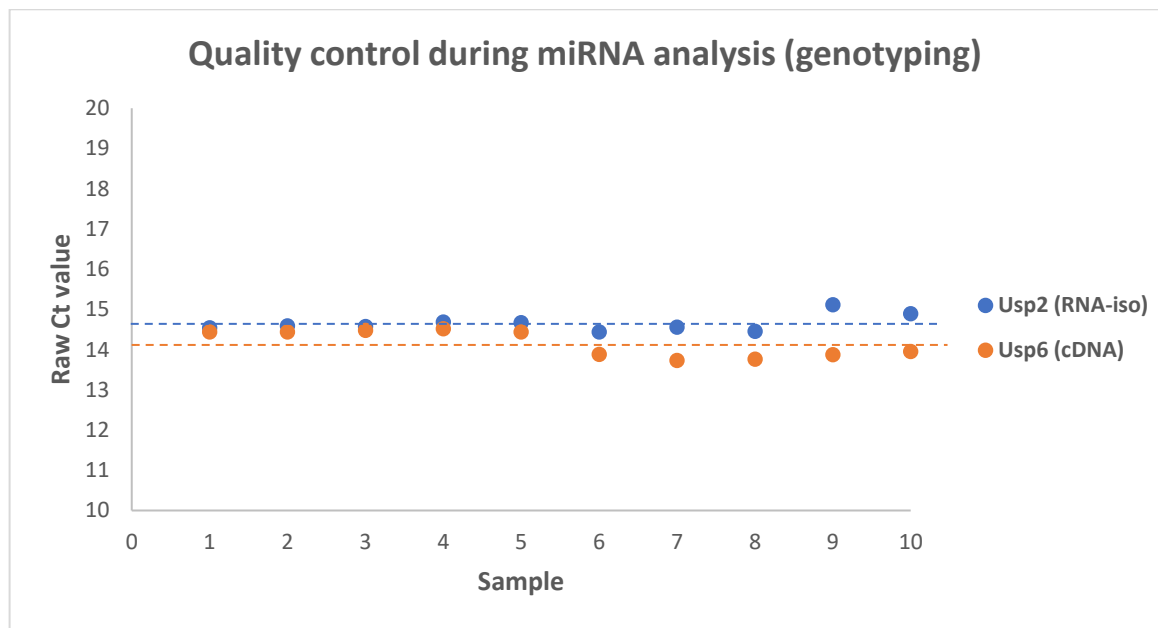


Figure 13: Quality control of each technical operation during genotyping. Usp2 was added during RNA isolation while Usp6 was spiked in during cDNA synthesis. The dashed line represents the respective mean value of each spike in control. Each datapoint corresponds to a single technical replicate.

4.3. Animal feeding experiment

After successfully evaluating that miR-21 is present in higher amounts in pasteurized milk than in UHT milk and furthermore establishing that the mice had indeed the correct genetic background, the feeding experiment was launched. According to the outlined scheme in the Material and Methods section (see *Table 7*) the mice were alternately fed with either UHT (used as internal matrix control) or PAS milk. All mice were fed parallelly in the same pattern and housed in the same cage.

After 3 days of miR-21-low UHT milk feed, the first blood sample was taken (T1). Then, mice were fed regular water for three days to ensure a washout of eventual miRNA uptake, before the next blood sample was taken (T2). The final blood samples were taken after 3 days of feeding pasteurized milk and resemble timepoint 3 (T3) in the uptake evaluation experiment. All samples had to be treated with heparinase prior to cDNA synthesis and qPCR – the assessment of the effect of heparin on the enzymatic reactions follows in the next chapter.

4.3.1. Negative effects of heparin on qPCR

As heparin has an inhibitory effect on enzymatic reactions during qPCR and cDNA synthesis, a degradation of heparin needed to be performed prior to miRNA analysis. Hence, bacterial heparinase was utilized to digest heparin in the heparin plasma samples.

To give an insight on the effect of heparin on the experiment, the same qPCR was performed prior and after heparinase digestion. The respective quality control (*Usp2*) values of both experiments is shown in the following figure (*Figure 14*).

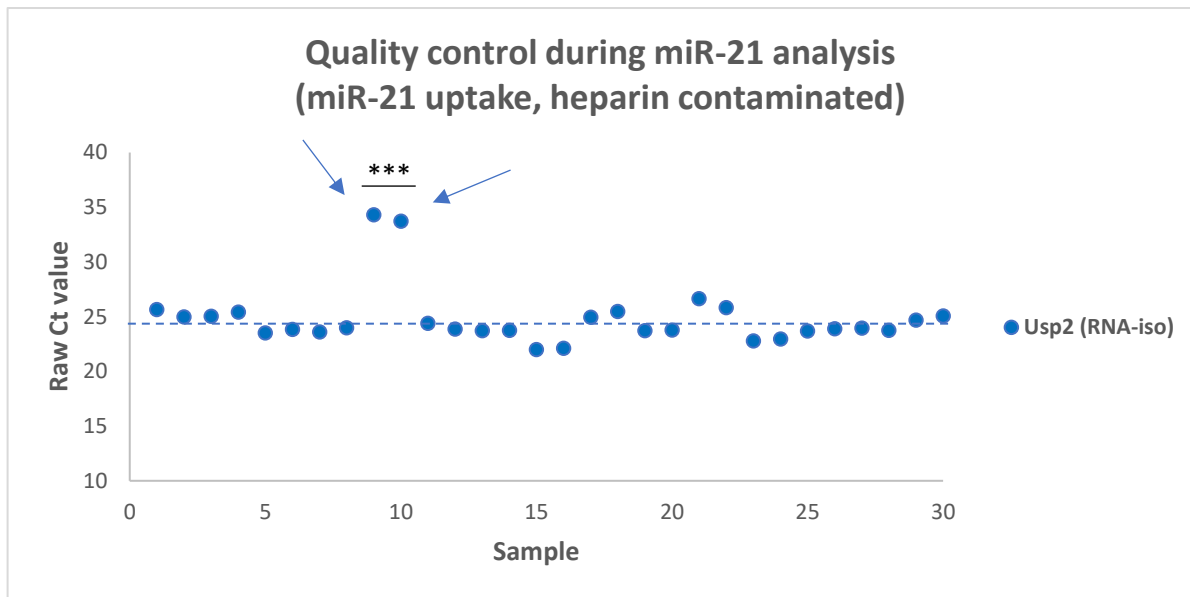


Figure 14: Evaluation of quality of miR-21 uptake analysis without heparinase treatment. Usp2 was added during RNA isolation and used as sole quality control spike in. The dashed line represents the respective mean value of Usp2. Each datapoint corresponds to a single technical replicate. Arrow marked samples indicate outliers prone to elimination.

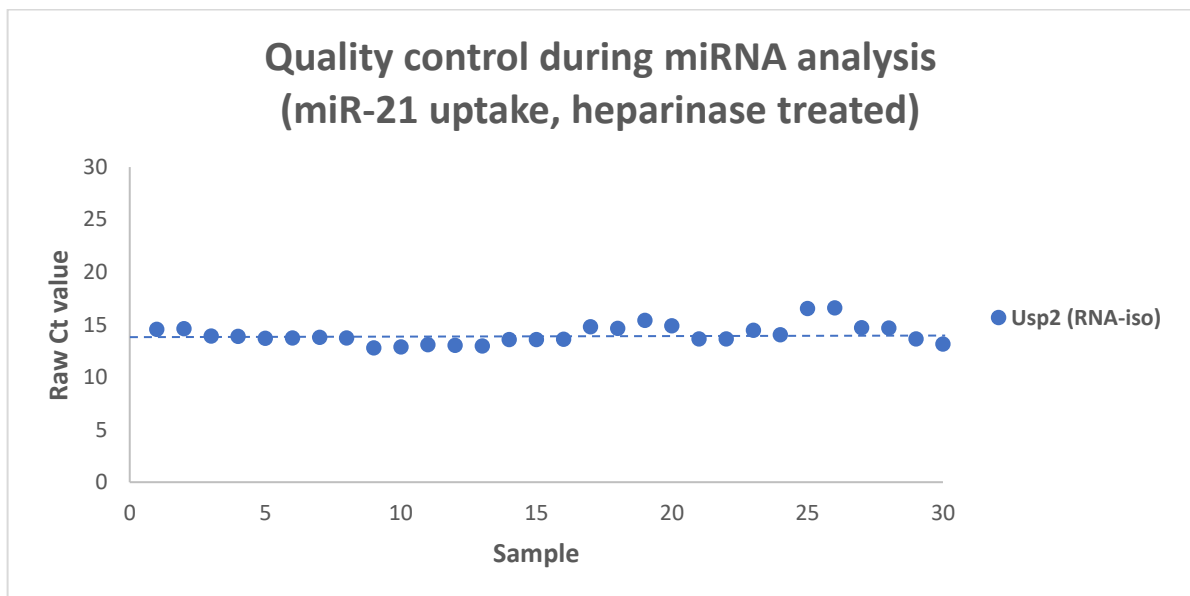


Figure 15: Evaluation of quality of miR-21 uptake analysis with heparinase treatment.. Usp2 was added during RNA isolation and used as sole quality control spike in. The dashed line represents the respective mean value of Usp2. Each datapoint corresponds to a single technical replicate.

As can be seen in Figure 14 and 15, the spread around the mean raw Ct value is higher in samples without heparinase treatment than in those treated (standard deviation of 2.66 vs 0.93, respectively). Additionally, two samples needed to be excluded (sample 9 and 10, marked with arrows). Moreover, the mean Ct value of 24.85 was also roughly 10.7 cycles over the heparinase treated control value (14.10). In consequence, this led to an apparent

calculated reduction in copy number of a factor of 1663 in the same samples ($2^{10.7}$). These findings highlight the importance of avoiding heparin plasma, when working with DNA, RNA or micro-RNAs, as heparin binds on such molecules irreversibly and therefore inhibits polymerase activity. If heparin plasma cannot be avoided, heparinase treatment is an effective method to elimination heparin contaminations before further analysis steps.

4.3.2. Analysis of uptake of miR-21 into the murine bloodstream

After all blood samples from the different feeding timepoints were collected, processing and analysis of miR-21 levels was performed. The obtained Ct-values were again normalized to Usp2 and visualized (see *Figure 16*).

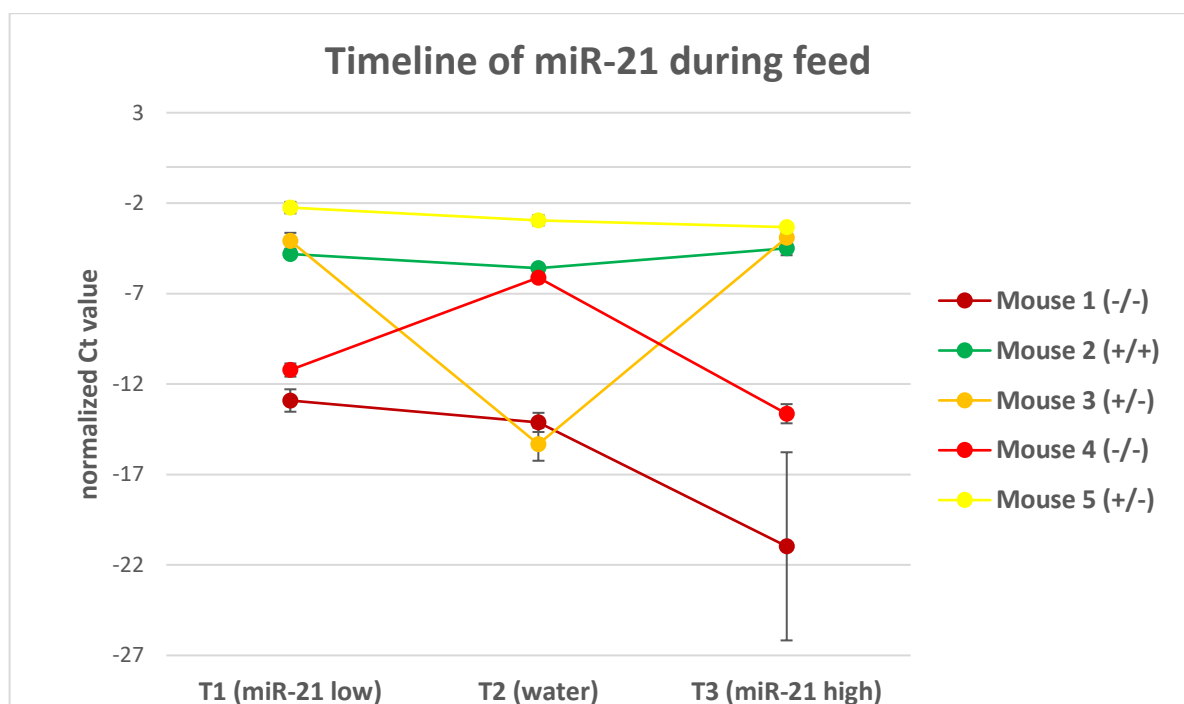


Figure 16: Normalized Ct values of miR-21 in murine blood over duration of the feeding experiment. Mice were fed with UHT milk for three days (timepoint 1), followed by three days of water feed (timepoint 2) and concluded by three days of pasteurized milk feed.

No increase in miR-21 levels could be shown over the duration of the experiment. On the contrary, a small linear decline in miR-21 levels could be observed in each mouse, except for mouse 3. Also, the initial miR-21 levels (T1) were not exceeded by any mouse after feed with miR-21 rich milk (T3), indicating that miR-21 is not accumulating in the murine circulatory system. Non-template controls gave no fluorescence signal.

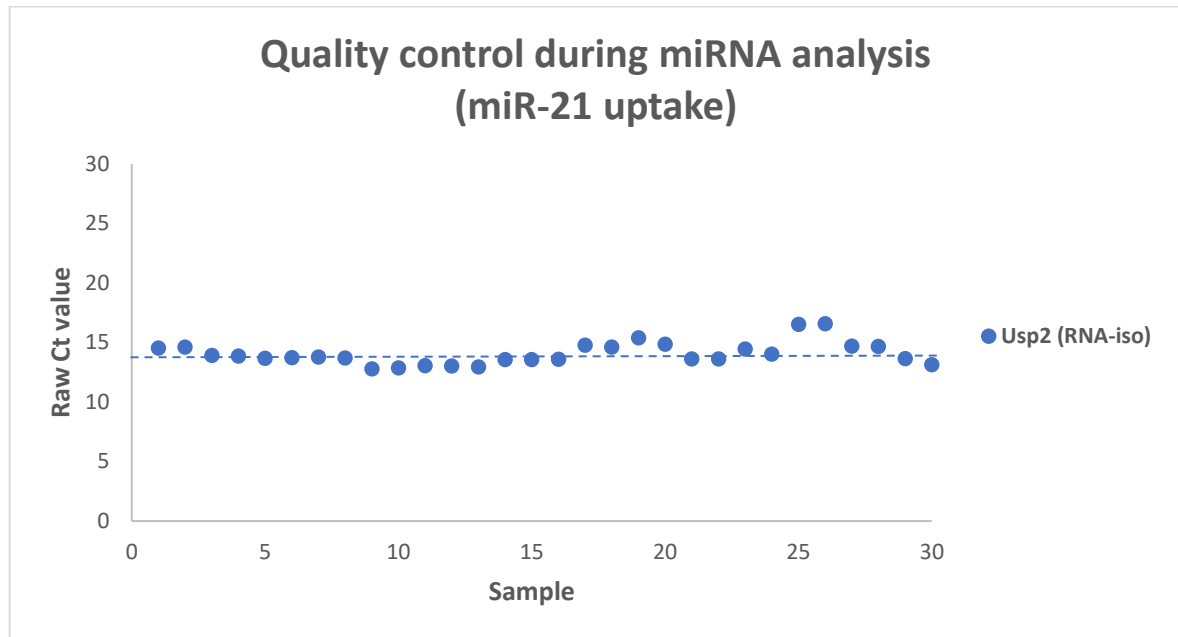


Figure 17: Evaluation of quality of miR-21 uptake analysis. Usp2 was added during RNA isolation and used as sole quality control spike in. The dashed line represents the respective mean value of Usp2. Each datapoint corresponds to a single technical replicate.

In Figure 17, the quality control of the feeding experiment analysis can be seen, showing a regular spread around the mean raw Ct value of 14.1, with a maximum of 16.5 and a minimum of 12.7. Due to the high number of samples, longer processing time and hence degradation of micro-RNAs seem to have influenced the quality of the experiment in a negative way, as can be seen by the higher deviation from the expected raw Ct baseline of samples 20-30. As the spread was not significantly increased and the normalization of each technical replicate was performed on its internal synthetic spike in, no samples needed to be eliminated or evaluated again.

4.3.3. Analysis of miR-21 uptake in liver and small intestine

After studying the results from the blood samples of the timeline experiment, we could safely assume that miR-21 is not accumulating in the murine bloodstream during milk feed. Consequentially, we decided to quantify the miRNA-21 content of the small intestine and the liver to gain insight if miRNA-21 eventually accumulated in the tissue throughout the experiment. For this reason, total DNA was isolated from tissue and used for qPCR amplification. Raw Ct values were normalized to an endogenous, highly conserved gene, U6 spliceosomal RNA (U6 snRNA).

This experiment was limited in its significance, as we could not study a timeline dependent concentration of miR-21 but only the endpoint amount in the respective organs. For this reason, we set a limit of detection (LOD), which was empirically documented by many qPCR related studies to be in the region of raw Ct = 35. The theoretical background of this hypothesis is that after a certain number of cycles, a phenomenon called Poisson noise starts to gain in impact by generating unspecific fluorescent signal.

As can be seen in *Figure 18*, *mir-21* levels in knockout mouse could not be re-supplemented to heterozygous/wildtype levels. However, and in comparison with the control groups, there was a higher spread of data points around the limit of detection. Since the experimental setting didn't include a non-treated knock-out mouse group for reference levels of miR-21 in liver and intestine, it remains unclear if the spread visualizes a small uptake of miR-21 into organs or reflects increased background noise around LOD.

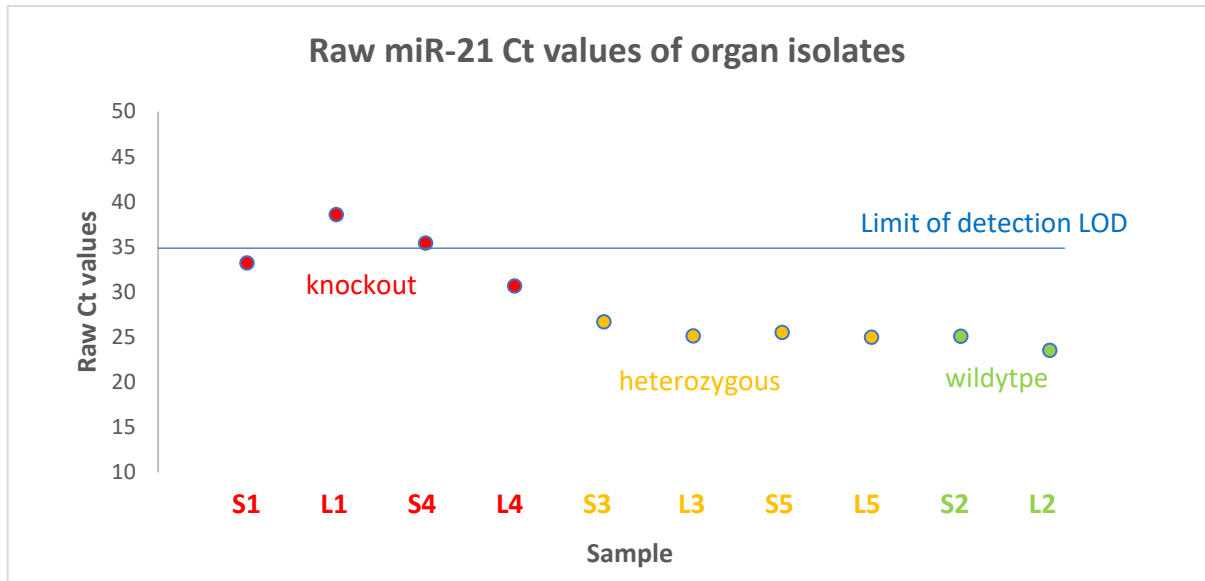


Figure 18: Visualization of raw miR-21 values of organ isolates: The respective colors show the genotype of the sample (red = knockout, orange = heterozygous, green = wildtype). Special attention is given to the first 4 samples (Mouse 1 Intestine, Mouse 1 Liver, Mouse 4 Intestine, Mouse 4 Liver) which are in the region of the limit of detection (LOD) of the qPCR reaction.

In the next step, we normalized the raw data points to U6 snRNA to study the differences of terminal miR-21 concentration between the different genotypes, Figure 19 and 20 represent these differences visually. A Ct difference around 8-9 could be observed between knockout and wildtype/heterozygous genotype with a resulting difference of factor 360 in miR-21 amount in both liver and small intestine.

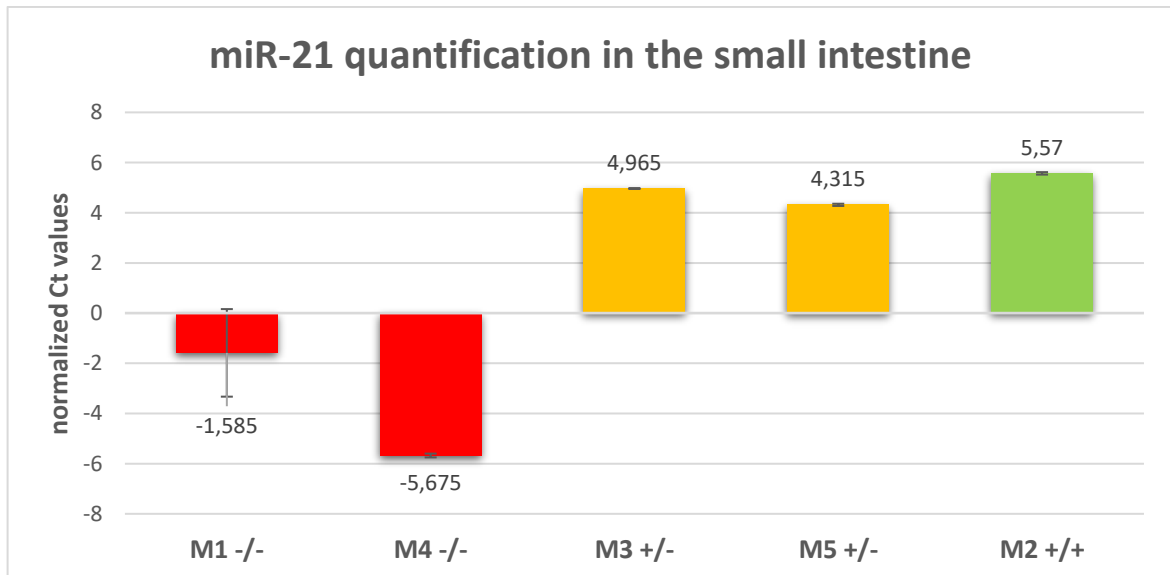


Figure 19: Visualization of final miR-21 levels in the small intestine. 5 ng of total cDNA were amplified in a qPCR reaction and the obtained Ct values were normalized to U6 snRNA. (M1, stands for mouse 1, M4 for mouse 4, etc.)

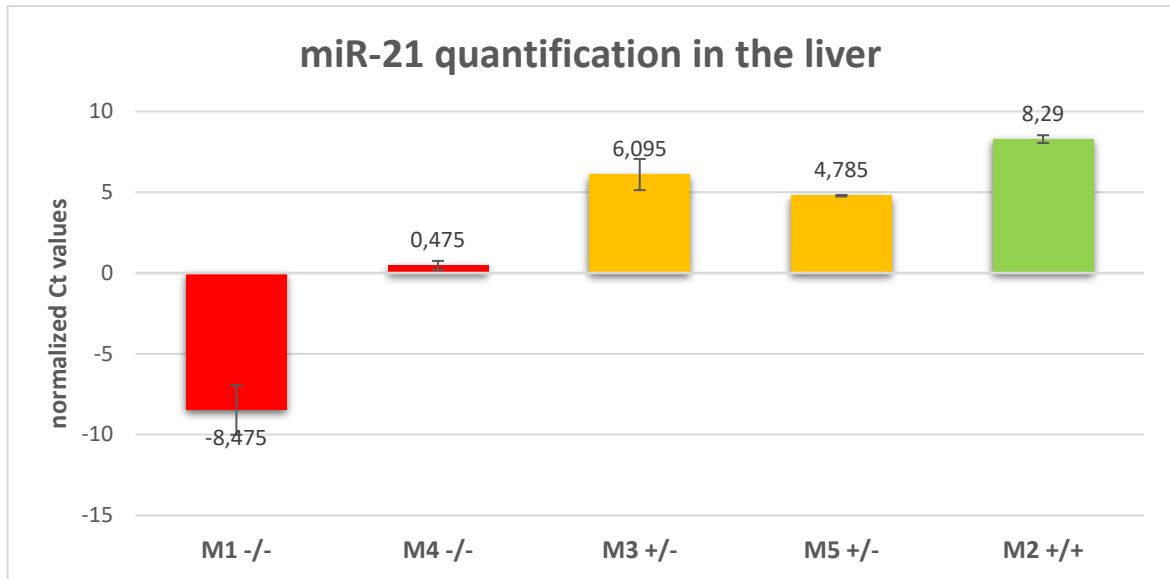


Figure 20: Visualization of final miR-21 levels in the liver. 5 ng of total cDNA were amplified in a qPCR reaction and the obtained Ct values were normalized to U6 snRNA. (M1, stands for mouse 1, M4 for mouse 4, etc.)

Again, a quality check was performed by plotting the raw Ct datapoints of U6 snRNA into a dot graph and visualizing the mean. In both organs, small intestine (Figure 21) and liver (Figure 22), U6 snRNA was evenly distributed and no outliers were detected. Secondly, U6 snRNA was stably expressed in both organs and the expression levels were similar, indicating that U6 snRNA is indeed a valid reference gene to analyze micro-RNA expression in those organs.

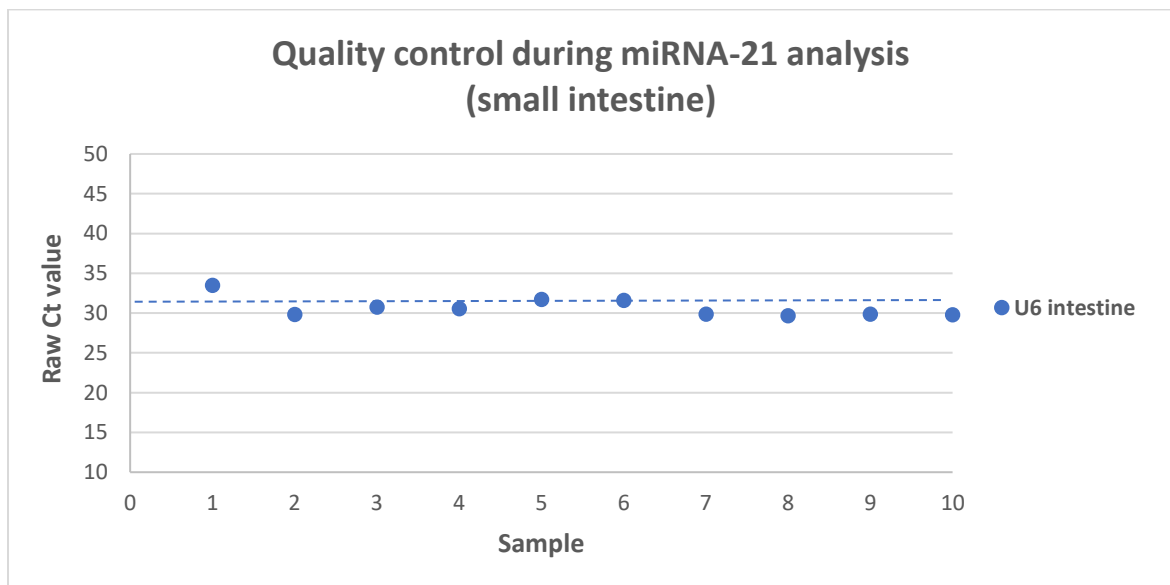


Figure 21: Evaluation of quality of miR-21 uptake analysis in the small intestine. U6 snRNA is an endogenously and stably expressed control gene used for normalization of miRNA values in organs. The

dashed line represents the respective mean value of U6. Each datapoint corresponds to a single technical replicate.

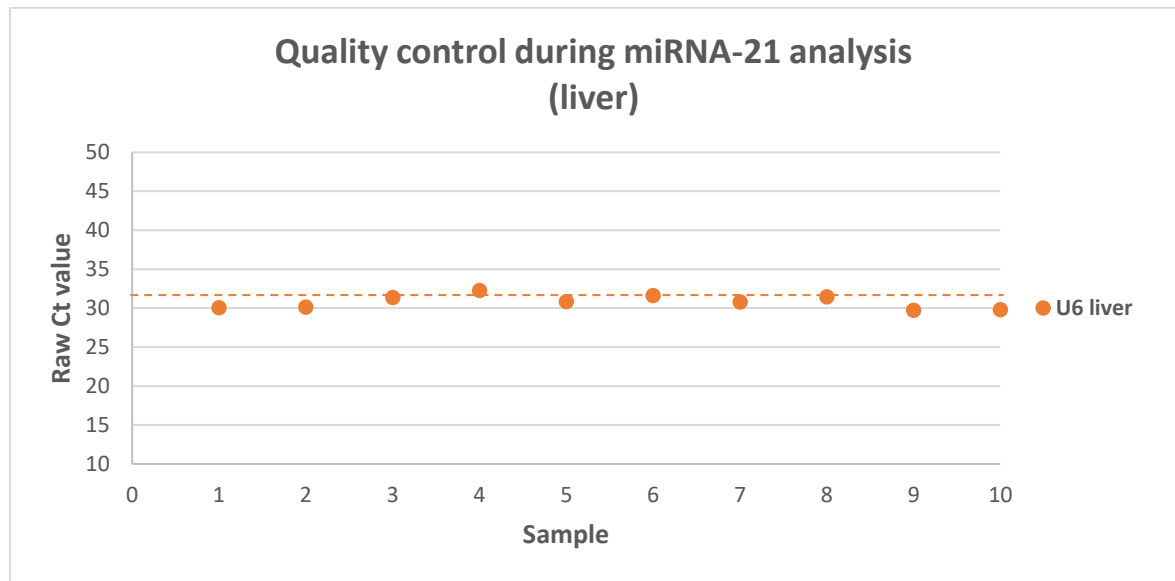


Figure 22: Evaluation of quality of miR-21 uptake analysis in the liver. U6 snRNA is an endogenously and stably expressed control gene used for normalization of miRNA values in organs. The dashed line represents the respective mean value of U6. Each datapoint corresponds to a single technical replicate.

5. Discussion

5.1. Summary, key messages and questions

While the alternating feeding scheme experiment with low- and high-miRNA containing milk did not show any uptake of micro-RNAs into the murine bloodstream, the organ isolate experiment gave a small hint in the possibility of uptake and transport of these small non-coding elements into the metabolically important organs of the liver and small intestine. However, no definite statement could be made whether the signals were just noise or actual miRNA-specific signal. Moreover, no re-supplementation to the mir-21 levels of the control groups could be achieved. This leads to the belief and conclusion that dietary micro-RNAs (if at all taken up) serve only a nutritional but not a functional purpose, as they are either degraded and taken up or eliminated by the gastric tract.

Despite the negative results, some significant key messages and thought-provoking questions could still be distilled out of this experimental setup and the results can be a spark for further experiments and ideas:

- Pasteurized/untreated cow milk contains roughly 217 times more micro-RNAs than ultra-high-temperature treated cow milk making it a cheap and sustainable origin of micro-RNAs for versatile experiments
- However, is a 3-day milk feed enough for accumulation of micro-RNAs in the murine system and is this limited nourishment in consequence enough for eliciting effects on the genetic level? An adaptation of experimental setup and mouse genotypes and cohorts could pave deeper insights on the possibilities of micro-RNA uptake.
- Additionally, the age-dependent functional micro-RNA uptake hypothesis grows in significance: as we have shown, there is no definite uptake of micro-RNAs in adult mammals, but does this also count for the nursing offspring?
- In hindsight, mouse experiments might not be optimal for testing hypotheses on the outcome for human health. However, to date, there is no alternative model available.

During the conduct and analysis of this small research project, numerous tweaks, improvements and problems have arisen and will be discussed in the following outlook.

5.2. Outlook on experimental setup improvements and contrasting approaches in the study of miRNA-uptake

The uptake of EVs in the bloodstream through the gastric barrier remains a much-debated topic in the scientific world. A recent study (Munagala, Aqil, Jeybalan, & Gupta, 2016) has shown that bovine exosomal biomarkers can indeed be quantified in rat tissue and organs after feed with labelled exosomes (A19-93M diet) both intravenously and orally and that those vesicles did not elicit an immunological or inflammatory response. An inflammatory response would have been a valid postulation for the outcome of our experiments: A murine immunological barrier reaction to bovine exosomes and in consequence a rejection of these vesicles and their respective cargo could have been a reason why no

extrinsic micro-RNA signal had been detected in our research. However, with the outcomes of the above study, a partial intestinal degradation of dietary miRNAs cannot be excluded and should be followed upon on.

Concerning the experimental setup, an increase in animal sample size as well as addition of mock-treated control groups would help to overcome the heterogeneity between the murine individuals and help to increase the statistical power of this study. In this experiment, we only had five middle-aged mice with different genetic background available. A study with different, bigger mouse cohorts could eradicate the problem: A cohort of mixed genotype (wt, het, ko) which only receives water, a cohort of the same makeup which only receives pasteurized cow milk and a cohort which receives UHT cow milk could be established to provide a decent sample size with a viable amount of controls and in consequence to detect significant trends. However, if there was a striking difference after the different feeding strategies, it should have been possible to be observed even in our pilot study with two animals.

Hence, the question arose if a 3-day feed interval could be too short for the micro-RNAs to accumulate in the murine system and give a definite signal in downstream analysis. To determine long-term effect of micro-RNA feed, feeding interval could be increased. Regular blood draws and comparison of miR-21 levels in plasma between the different cohorts and genotypes can then be conducted over several months. This approach could possibly be more conclusive to the final answer whether micro-RNAs are taken up through the gastrointestinal tract and also if the prolonged saturation of the circulatory system can counteract the high turnover rates and relatively small half-lives of circulating micro-RNAs (Bail, et al., 2010).

Another important factor which could have significant influence on the mechanism of miRNA uptake is the age of the mice. As postulated in the age-dependent functional hypothesis of miRNA-uptake, the intestinal barrier might be passable for milk-derived EVs packed with these regulatory nucleic acids in the postnatal/young phase leading to an extensive growth stimulus for the youngling. To study this effect, a miR-21 wt adult female mouse could breastfeed a miR-21 ko brood with a wt offspring as control. The timeline for the experiment would be shorter, as the lactation period for mice only lasts up to 16 days

(König & Markl, 1987) but potential cross-species immunogenicity issues like elimination of extrinsic exosomal particles would be resolved.

Nevertheless, quantification of circulatory micro-RNAs remains a double-edged sword: Extrinsic factors like stress (Olejniczak, Kotowska-Zimmer, & Krzyzosiak, 2018), disease (as shown in the introduction of the thesis) and nutrition may disturb the physiological miRNA levels in the body and might deliver a bias when interpreting circulatory microRNA concentrations. To support such data, downstream biomolecular methods like Western Blot of miRNA-targets would be necessary. As previously discussed, lactation with a high content of micro-RNAs could potentially regulate cellular signaling cascades like the Akt-pathway. By comparison of UHT-fed and PAS-fed murine protein signatures (e.g. quantification of key proteins from the Akt pathway in the liver), one could visualize in a Western Blot if a reduction or increase of these specific proteins occurs on a cellular level after continuous feed with the respective milk variant. For example, and as discussed in the introduction, a reduction of PTEN should be observed after feed with high-miRNA 21 containing milk, as PTEN is specifically downregulated by miR-21.

The study of micro-RNAs remains a fascinating field in the scientific world and many obstacles still need to be overcome when performing and interpreting the experiments and the resulting data. Delivery of specific micro-RNAs or targeting micro-RNAs are on the verge to evolve into a new branch of biological therapeutics, however a lot of research still needs to be conducted to evaluate efficacy and safety of this novel treatment methods.

It remains a huge controversy, whether micro-RNAs are taken up by the gastric system and are distributed internally by the circulatory system. There are many scientifically sound papers on both ends of this discussion and the next months and years will be decisive whether a research group will eventually draw a conclusion to the “micro-RNA uptake from milk” myth, whether it will be a good or bad one for the milk industry.

6. References

- Alberts, Johnson, & Lewis. (2002). *Molecular Biology of the Cell. 4th edition*. Garland Science.
- Alsaweed, e. a. (2015). MicroRNAs in Breastmilk and the Lactating Breast: Potential Immunoprotectors and Developmental Regulators for the Infant and the Mother. *Int J Environ Res Public Health (Vol. 12)*.
- Asangani, I. A. (2007). MicroRNA-21 (miR-21) post-transcriptionally downregulates tumor suppressor Pdc4 and stimulates invasion, intravasation and metastasis in colorectal cancer. *Oncogene (Vol. 27)*.
- Bail, S., Swerdel, M., Liu, H., Jiao, X., Goff, L., Hart, R., & Kiledjian, M. (2010). Differential regulation of microRNA stability. *RNA (Vol. 16)*.
- Bartel, D. P. (2004). MicroRNAs: Genomics, Biogenesis, Mechanism, and Function. *Cell (Vol. 116)*.
- Benhamed, e. (2012). Senescence is an Endogenous Trigger for microRNA-Directed Transcriptional Gene Silencing in Human Cells. *Nat Cell Biol (Vol. 14)*.
- Benmoussa, e. a. (2016). Commercial Dairy Cow Milk microRNAs Resist Digestion under Simulated Gastrointestinal Tract Conditions. *Journal of Nutrition (Vol. 146)*.
- Bentwich, e. (2005). Identification of hundreds of conserved and nonconserved human microRNAs. *Nat. Genet. (Vol. 37)*.
- Bitesizebio.com. (2019). *bitesizebio.com*. Retrieved from BiteSize Bio.
- Blondal, e. a. (2013). Assessing sample and miRNA profile quality in serum and plasma or other biofluids. *Methods (Vol. 59)*.
- Bullrich, F., & Croce, C. M. (2001). CLL. *Chronic Lymphoid Leukemias*.
- Cairns, Okami, & Halachmi. (1997). Frequent inactivation of PTEN/MMAC1 in primary prostate cancer. *Cancer Res (Vol. 57)*.
- Chu, E. C., & Tarnawski, A. S. (2004). PTEN regulatory functions in tumor suppression. *Med Sci Monit (Vol. 10)*.
- Concepcion, C. (2012). The miR-17-92 family of microRNA clusters in development and disease. *Cancer J (Vol. 18)*.
- Coussens, L., & Werb, Z. (2002). Inflammation and cancer. *Nature (Vol. 420)*.
- Dews, M. (2006). Augmentation of tumor angiogenesis by a Myc-activated microRNA cluster. *Nat. Genet. (Vol. 38)*.
- Dranoff, G. (2014). Cytokines in cancer pathogenesis and cancer therapy. *Nat Rev Cancer (Vol. 4)*.
- E Lund, e. (2004). Nuclear export of microRNA precursors. *Science (Vol. 303)*.
- Eis, & Tam. (2005). Accumulation of miR-155 and BIC RNA in human B cell lymphomas. *Proc Natl Acad Sci USA (Vol. 102)*.
- Gantier, e. (2011). Analysis of microRNA turnover in mammalian cells following Dicer1 ablation. *Nucleic Acids Res (Vol. 39)*.

- György. (2011). Membrane vesicles, current state-of-the-art: emerging role of extracellular vesicles. *Cellular and Molecular Life Sciences (Vol. 68)*.
- He, & Thomson. (2005). A microRNA polycistron as a potential human oncogene. *Nature (Vol. 435)*.
- He, L., & Hannon, G. J. (2004). Erratum: MicroRNAs: small RNAs with a big role in gene regulation. *Nature Rev. Gen.*
- Hunter, M. (2008). Detection of microRNA Expression in Human Peripheral Blood Microvesicle. *PLoS One (Vol. 3)*.
- Jang, M. H. (2017). Prognostic value of microRNA-9 and microRNA-155 expression in triple-negative breast cancer. *Human Pathology (Vol. 68)*.
- JE Braun, e. (2012). A direct interaction between DCP1 and XRN1 couples mRNA decapping to 5' exonucleolytic degradation. *Nat Struct Mol Biol (Vol. 19)*.
- Jo, M. H. (2015). Human Argonaute 2 Has Diverse Reaction Pathways on Target RNAs. *Molecular Cell (Vol. 59)*.
- Kim, V. (2005). Small RNAs: classification, biogenesis, and function. *Mol. Cells (Vol. 19)*.
- Kinet, H. D. (2013). Cardiovascular extracellular microRNAs: emerging diagnostic markers and mechanisms of cell-to-cell RNA communication. *Front Genet (Vol. 4)*.
- Kirchner, e. a. (2016). microRNA in native and processed cow's milk and its implication for the farm milk effect on asthma. *J Allergy Clin Immunol*.
- König, B., & Markl, H. (1987). Maternal care in house mice. *Behavioral Ecology and Sociobiology (Vol. 20)*.
- Kumarswamy, R., Volkmann, I., & Thum, T. (2011). Regulation and function of miRNA-21 in health and. *RNA Biol. (Vol. 8)*.
- Lee, Rhonda, Feinbaum, & Ambros. (1993). The C. elegans Heterochronic Gene lin-4. *Cell (Vol. 75)*.
- Lee, Y. (2002). MicroRNA maturation: stepwise processing and subcellular localization. *EMBO J (Vol. 21)*.
- Li, & Kowdley. (2012). MicroRNAs in Common Human Diseases. *Genomics, Proteomics and Bioinformatics (Vol. 10)*.
- Lu, J. (2005). MicroRNA expression profiles classify human cancers. *Nature (Vol. 435)*.
- Lu, Y.-C., Yeh, W.-C., & Ohashi, P. (2008). LPS/TLR4 signal transduction pathway. *Cytokine (Vol. 42)*.
- Macierzanka, Mackie, Bajka, Rigby, Nau, & Dupont. (2014). Transport of particles in intestinal mucus under simulated infant and adult physiological conditions: impact of mucus structure and extracellular DNA. *PLoS One (Vol. 9)*.
- Martin, & Caplen. (2007). Applications of RNA. *Annu. Rev. Genomics Hum. Genet. .*
- Melnik, B. (2016). Milk miRNAs: simple nutrients or systemic functional regulators? *Nutrition and Metabolism (Vol. 13)*.

- Meng, F., Roger, H., Wehbe-Jane, H., Kalpana, G., Samson, J., & Tushar, P. (2007). MicroRNA-21 Regulates Expression of the PTEN Tumor Suppressor Gene in Human Hepatocellular Cancer. *Gastroenterology (Vol. 133)*.
- Mu, & Han. (2009). Genetic dissection of the miR-17~92 cluster of microRNAs in Myc-induced B-cell lymphomas. *Genes Dev. (Vol. 23)*.
- Mulcahy. (2014). Routes and mechanisms of extracellular vesicle uptake. *J Extracell vesicles (Vol. 3)*.
- Munagala, Aqil, Jeybalan, & Gupta. (2016). Bovine milk-derived exosomes for drug delivery. *Cancer Letters (Vol. 371)*.
- Olejniczak, Kotowska-Zimmer, & Krzyzosiak. (2018). Stress-induced changes in miRNA biogenesis and functioning. *Cell Mol Life Sci (Vol. 75)*.
- Oswald, N. (2018). *BiteSizeBio*. Retrieved from BiteSizeBio.
- Rasmussen, e. a. (2010). *J. Exp. Med. (Vol. 207)*.
- Robbins, & Morelli. (2014). Regulation of Immune Responses by Extracellular Vesicles. *Nat Rev Immunol (Vol. 14)*.
- Roderburg, & Luedde. (2014). Circulating microRNAs as markers of liver inflammation, fibrosis and cancer. *J Hepatol (Vol. 61)*.
- Ruby, Jan, & Bartel. (2007). Intronic microRNA precursors that bypass Drosha processing. *Nature (Vol. 448)*.
- Smith-Vikos, & Slack. (2012). MicroRNAs and their roles in aging. *J Cell Sci (Vol. 125)*.
- Takeda, K., & Shizuo, A. (2005). Toll-like receptors in innate immunity . *International Immunology (Vol. 17)*.
- Tanzer, & Stadler. (2004). Molecular evolution of a microRNA cluster. *J Mol Biol. (2004). J Mol Biol. (Vol 339)*.
- Tao, Y. (2018). Role of miR-155 in immune regulation and its relevance in oral lichen planus (Review). *Experimental and Therapeutic Medicine (Vol. 17)*.
- Wang. (2012). Comparing the MicroRNA Spectrum between Serum and Plasma. *PLoS One (Vol. 7)*.
- Wang, P. (2010). Inducible microRNA-155 Feedback Promotes Type I IFN Signaling in Antiviral Innate Immunity by Targeting Suppressor of Cytokine Signaling 1. *The Journal of Immunology (Vol. 185)*.
- Wang, Puc, & Li. (1997). Somatic mutations of PTEN in glioblastoma. *Cancer Res (Vol. 57)*.
- Wightman, Ha, & Ruvkun. (1993). Posttranscriptional regulation of the heterochronic gene lin-14 by lin-4 mediates temporal pattern formation in *C. elegans*. *Cell (Vol. 75)*.
- Yàñez-Mo. (2015). Biological properties of extracellular vesicles and their physiological functions. *J Extracell vesicles (Vol. 4)*.
- Yang, Yu, Huang, Li, He, & Li. (2013). miR-21 confers cisplatin resistance in gastric cancer cells by regulating PTEN. *Toxicology (Vol. 306)*.
- Yoda, e. (2010). ATP-dependent human RISC assembly pathways. *Nat Struct Mol Biol. (Vol. 17)*.

Zhou, Q., & Li, M. (2012). Immune-related MicroRNAs are Abundant in Breast Milk Exosomes. *Int J Biol Sci* (Vol. 8).

7. Appendix

7.1. Abbreviations

%	percent
µl	microlitre
µM	micromolar
3'	three prime end
5'	five prime end
A	arginine
AGO	argonaute
Akt	protein kinase B
BAD	CL2 sociated agonist of cell death
B-CLL	B-cell lymphoma
bp	base pair
C	cytosine
C	concentration
Casp	caspase
c-DNA	complementary DNA
Cq/Ct	quantification cycle
CTGF	connective tissue growth factor
DC	dendritic cell
DCP2	mRNA-decapping enzyme 2
ddH ₂ O	double-distilled water
DNA	deoxyribonucleic acid
dNTP	deoxynucleoside triphosphate
ds	double strand
EDTA	ethylenediamine tetraacetic acid
EV	extracellular vesicle
g	gravitational acceleration
G	guanine
GMP	good manufacturing practice
GTP	guanosine 5'-triphosphate
h	hour
HCV	hepatitis C virus
HDL	high density lipoprotein
HIV	human immunodeficiency virus
Has	homo sapiens
INPP5K	inositol polyphosphatase-5-phosphatase
ko	knockout
kb	kilobase
let-7	letal-7 micro-RNA
LOD	limit of detection
LPS	lipopolysaccharide
m	mass

MDM2	mouse double minute 2 homolog
min	minute
miRISC	micro-RNA RISC complex
miRNA	micro-RNA
miRNP	micro ribonucleoprotein complex
ml	millilitre
mM	millimolar
mmol	millimole
mmu	mus musculus
mRNA	messenger RNA
MRE	micro-RNA response element
mTOR	mammalian target of rapamycin
MVB	multivesicular body
Myc	avian myelocytomatosis viral oncogene homolog
NF- κ B	nuclear factor kappa-B
NFW	nuclease free water
NK	natural killer
nt	nucleotide
oncomiR	oncogenic micro-RNA
ORF	open reading frame
p21	cyclin-dependent kinase inhibitor 1
p53	cellular tumor antigen p53
PAMP	pathogen associated molecular patterns
PAS	pasteurized
PCR	polymerase chain reaction
PDCD4	programmed cell death protein 4
PDK1	phosphoinositide-dependent kinase-1
PI3K	phosphoinositide 3-kinase
PIP2	phosphatidylinositol 4,5-bisphosphate
PIP3	phosphatidylinositol (3,4,5)-trisphosphate
PTEN	phosphatase and tensin homolog
PTGS	post-transcriptional gene silencing
pre-miR	precursor miRNA
pri-miR	primary miRNA
pg	picogram
qPCR	quantitative polymerase chain reaction
Ran	androgen receptor-associated protein 24
Rb	retinoblastoma
RBP	retinol binding protein
RISC	RNA-induced silencing complex
RNA	ribonucleic acid
RNAse	ribonuclease
RT	reverse transcription
RT	room temperature
RT-qPCR	real-time qPCR
sec	seconds

siRNA	small interfering RNA
snRNA	small non-coding RNA
SOCS1	suppressor of cytokine signaling 1
SOP	standard operating procedure
T	thymidine
TAR	transactivation response element
TEM	transmission electron microscope
Th	t-helper
TLR	toll-like receptor
TNF- α	tumor necrosis factor alpha
Treg	t-regulatory
TSP	thrombospondin
Tyr	tyrosine
UTR	untranslated region
U	uracile
UHT	ultra-high temperature
Usp	universal spike-in
UV	ultraviolet
VIS	visible
wt	wildtype
XRN1	5'-3' exoribonuclease 1